# Fluid systems in foreland fold-and-thrust belts: on overview from the Southern Pyrennees

A. Travé, Pierre Labaume, J. Vergès

# Fluid Systems in Foreland Fold-and-Thrust Belts: An Overview from the Southern Pyrenees

**Travé, A. · Labaume, P. · Vergés, J.**

**Abstract.** The analysis of three different regions of the South-Pyrenean fold-and-thrust belt reveals that during the Tertiary compression the hydrological system was compartmentalised in time and space. During the early-middle Eocene, when the thrust front affected marine soft-sediments in the Ainsa basin, the thrust fault zones were dominated by formation fluids derived from Eocene marine waters trapped in the underlying Eocene marls, although influences of meteoric waters were also present. During the middle-late Eocene, when the thrust front emplaced marine rocks over continental redbeds in the eastern Catalan basin (L'Escala thrust), the thrust fault zones were dominated by meteoric fluids. These fluids flowed preferentially along these faults, draining laterally the meteoric fluids and acting as barriers hindering their flowing towards more external parts of the belt. During the Oligocene, the most external part of the fold-and-thrust belt in the eastern Catalan basin developed on top of a salt detachment horizon. The thrust front affected continental materials of late Eocene-Oligocene age. At this moment, the thrusts were conduits for meteoric fluids arriving from the surface and also for evolved meteoric fluids migrating over short distance upwards after being in contact with the underlying evaporitic beds.

Most of the fractures show a similar sequence of microfractures. Microfractures of stage 1 formed when the sediment was poorly lithified. Microfractures of stage 2 represent the main episode of vein formation which developed when a progressive induration of the host sediment occurred. During microfracture stage 3, formed in an extensional regime, the host sediment was more indurated. The repetition of this sequence of microfractures in different fracture generations of the same outcrop indicates that the sediment induration was restricted to the vicinity of the vein. Away from the veins, the sediment remained poorly lithified during the entire deformation cycle. Calcite cement within the host rock precipitated later than the syn-compressive veins, when the sediment was more indurated.

Elemental geochemistry and stable isotopes of the calcite veins indicates that early generation of microfractures is infilled by local fluids (either marine or meteoric), whereas external fluids (meteoric or evolved meteoric) infilled the main compressive stage of microfractures. The hot temperature of these fluids (157ºC to 183ºC in the Atiart-Arro example) indicates their circulation through deep parts of the thrust belt. The progressive increase of the $^{87}Sr/^{86}Sr$ ratio through time is due to the progressive uplift, exposure and erosion of the internal Pyrenean Axial Zone.

## 1 Introduction

Geofluids are related to the formation and deformation of the fold-and-thrust belts and sedimentary foreland basins. The geodynamic evolution of the belt - foreland basin system moves geofluids and, in their turn, geofluids condition the geodynamic evolution of the system by controlling the propagation of fractures and faults and the dynamics of fault activity. The fluid sources are likely to change during this coupled evolution, in particular because most foreland basins evolve from marine and largely underfilled to continenta overfilled and largely bypassing (e.g. Allen et al., 1986) (Fig. 1). Fractures and faults may have a major control on fluid distribution and migration pathways, acting as barriers or as conduits. The etailed petrology of the vein filling fractures, coupled with their distribution, geometry and microstructural study, is a key to understanding the coupling between fractures, faults and fluid, in particular 1) the mechanisms and kinematics of fluid-deformation relationships, 2) the fluid flow events and their relative timing, and 3) the synchronism, or not, between fracturation and fluid flow. The geochemical composition of the fracture-filling minerals and their comparison with the geochemistry and mineralogy of their host rocks allow to assess 1) the physico-chemical characteristics of the fluid, and therefore the fluid type and origin, 2) the degree of fluid/rock interaction (high versus low), 3) the type of fluid flow regime (closed versus open), and 4) the fluid pathways (pervasive versus channelized). Finally, the integration of all these data within a specific geological setting constrains the relative timing of fluid flow and the fluid driving force.

The main fluid flow systems in foreland-orogen contexts are driven by tectonics (Oliver, 1986; Burkhard & Kerrich, 1988; Machel & Cavell, 1999) and topography (Garven 1985, 1989, 1995). Structural and microstructural study of faults related to compression indicates

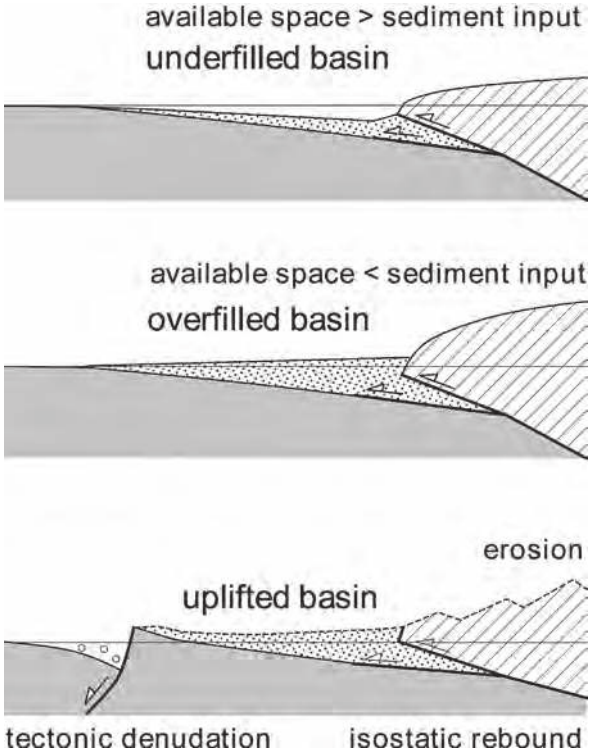


**Fig. 1.** Evolution of a foreland basin from marine and largely underfilled to continental. overfilled and largely bypassing. Post-orogenic vertical motions are mainly controlled by the interplay between tectonic and surficial denudation with concomitant isostatic rebound.

that a high-fluid pressure highly favours thrusting (Roure et al., 1994, 2005) although it is not a prerequisite (Dietrich et al., 1983; Cosgrove, 1993). Orogenic compression may drive fluid migration directly (Oliver, 1986), and significant fluid flow may migrate towards the foreland coevally with thrusting (Ge and Garven, 1992; Qing & Mountjoy, 1992). Bradbury & Woodwell (1987) inferred that each thrust sheet acted as a separate hydrodynamic unit for expulsion of fluids into the foreland. Geochemical studies of calcite cements in compressive fault zones indicate in some cases high fluid-rock interaction and relatively closed palaeohydrogeological regime (Dietrich et al., 1983; Budai, 1985; Kyser & Kerrich, 1990; Muchez et al., 1995; Calvet et al., 1996; Travé et al., 1997, 1998; Ferket et al., 2004) but, in other cases calcite cements indicate low fluid-rock interaction and relatively open palaeohydrogeological regime (Burkhard & Kerrich, 1988; Marquer & Burkhard, 1992). Quantitative modelling of fluid migration in active foreland basins reveals that fluid flow derived from basin sediment compaction is subordinate to that resulting from the rising hinterland topographic relief of the orogen (Ge & Garven, 1992; Bethke & Marshak, 1990; Bitzer et al., 1998). Ge & Garven (1994) calculated that the total volume of fluid expelled during thrusting is in the order of 1% of the total volume of pore fluid that moved through the section after thrusting (i.e., by topographically-driven flow), and these fluids did not travel more than a few km into the foreland. Low fluxes of tectonically-expelled fluids are also indicated in the Rocky Mountain Foreland Basin (Machel & Cavell, 1999) and in the Variscan foreland because recrystallization and lithification of the host rocks occurred earlier than thrusting (Muchez et al., 1995).

The South-Pyrenean fold-and-thrust belt represents an ideal natural fi ld laboratory for the study of fluid migration during orogenic compression because the evolution of the foreland basin from marine underfilled to continental overfilled and the coupled thrust front propagation are particularly well recorded. The aims of this paper are to compare the type and origin of the synkinematic fluids and the type of palaeohydrogeological regime at diff rent moments of the thrust front propagation. For this, we use data from three areas in three diff rent parts of the belt representative of the main situations of the belt front during the main tectonic events: the Atiart-Arro thrust-fold system in the Ainsa basin, and the L'Escala thrust and El Guix anticline, both located in the eastern Catalan basin (Fig. 2). Data from Atiart-Arro and El Guix are synthesised from detailed works already published separately elsewhere (Atiart-Arro: Travé et al., 1997, 1998; El Guix: Travé et al., 2000), whereas data from L'Escala are new data presented here for the first time. Details of analytical techniques and methods, as well as the detailed petrology in the cases of Atiart-Arro and El Guix, are not presented in this paper and the readers are referred to the previouly published papers.

We will also discuss the place of oil migration in the fluid history from an example in the eastern Catalan basin (Caja et al., 2006), and compare fluid flow in the thrust front with that associated with the emplacement of basement thrust sheets in inner parts of the belt (Grant et al., 1990; Banks et al., 1991; McCaig et al., 1995).

## 2 South-Pyrenean Fold-and-Thrust Belt

The continental collision of Iberia and Europe produced the formation of the Pyrenean orogen with a partial subduction of the Iberian lithosphere to the north (Choukroune et al., 1989; Roure et al., 1989; Muñoz, 1992; Beaumont et al., 2000). Convergence began during the Campanian and most of compressional deformation ceased during the early Miocene. Two large flexural foreland basins formed on both sides of the growing mountain chain: the Aquitaine retroforeland and the Ebro foreland basins (Fig. 2). After an early

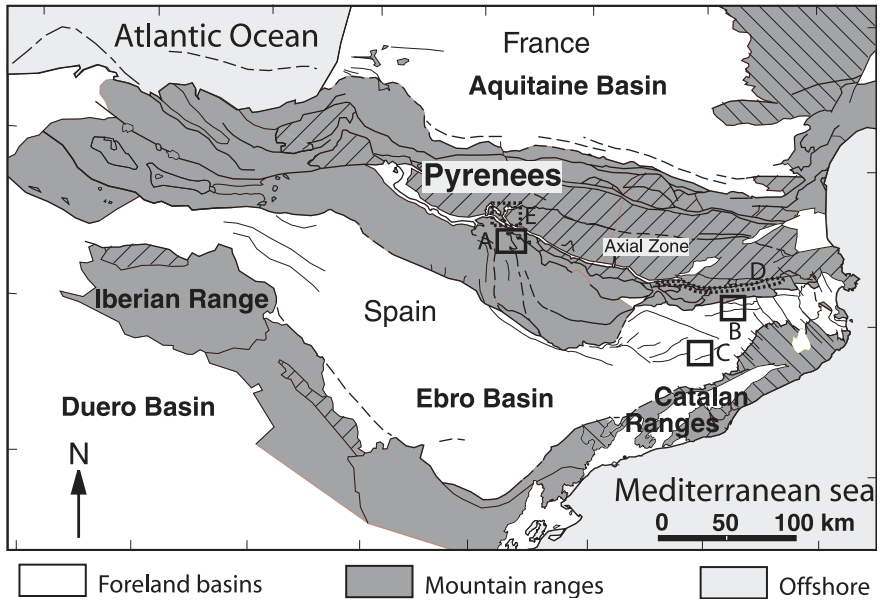


**Fig. 2.** Structural sketch of the Pyrenean belt and location of the studied outcrops. A: Atiart-Arro (early-middle Eocene); B: L'Escala (middle-late Eocene); C: El Guix (Oligocene); D: outcrop zone of Armanciès Formation marls (lower Eocene); E: outcrop area of Gavarnie basement thrust discussed in the text.

period of low subsidence rate and mainly continental or marine platform sedimentation, the South-Pyrenean foreland basin developed as underfilled and marine during the early-middle Eocene, with turbiditic troughs both in the eastermost and westernmost parts (the eastern Catalan and the Ainsa-Jaca basins, respectively). Subsequently, the basin became overfilled and continental from the middle-late Eocene to the end of shortening during the late Oligocene (Puigdefàbregas et al., 1986, 1992; Vergés et al., 1995, 1998). At the middle-upper Eocene boundary (~37 Ma) the uplift of the Western Pyrenees triggered the end of the marine foreland basin stage and originated an intermountain basin limited by the Pyrenees, the Catalan Coastal Ranges and the Iberian Range (Vergés & Burbank, 1996). An internal fluvial network delivered sediments to the Ebro Basin characterized by a large central lake (e.g., Anadón et al., 1979; Arenas & Pardo 1999). In the eastern Catalan basin, the deposition of the Cardona salts (~37 Ma) coincides with this transition from marine to continental conditions. The end of deformation along the South-Pyrenean thrust front occurred during the late Oligocene as determined by magnetostratigraphy on growth strata (~24.7 Ma) (Meigs et al., 1996). Fission track cooling ages in the Axial Zone of the central Pyrenees, however, reveal that basement uplift in the back of the fold-and-thrust belt ended its major uplift at about 30 Ma (Fitzgerald et al., 1999), and that younger movements occurred around 20 Ma along the southern edge of the Axial Zone (Sinclair et al., 2005; Campani et al., 2005). The Ebro basin infilled up to the late Miocene times when it was captured by Mediterranean rivers and thus ending its endorheic character (e.g., Coney et al., 1996; García-Castellanos et al., 2003).

During Pyrenean shortening there was a general migration of tectonic activity towards the foreland as well as of the sedimentary depocentres. Three main periods of thrust sheet movements can be diff rentiated with diff rent rates of motion (e.g. Vergés et al., 2002), namely:

1. An early period during the Late Cretaceous-Paleocene, related to the emplacement of the uppermost thrust sheets, with very low rates of about 0.5 mm/a;
2. A second period, during the early and middle Eocene, which is characterized by fast rates of thrust sheet emplacement in the order of 4.0 to 4.4 mm/a in submarine conditions;
3. During the third period (late Eocene – Oligocene) there was a decrease of the rates of thrust emplacement down to 1.5 to 2.6 mm/a.

The second and third periods largely coincide with the underfilled and overfilled stages of basin evolution, respectively.

The three selected structural domains (Fig. 2) to conduct this geofluid study are representative of the two last stages of the thrust front – foreland basin system migration. The Atiart-Arro fold-and-thrust system represents the submarine stage, during the early-middle Eocene. The L'Escala thrust represents an intermediate stage, during the middle-late Eocene in transitional marine-continental conditions. The El Guix anticline represents the latest stage, during the Oligocene, with continental conditions (Fig. 3).

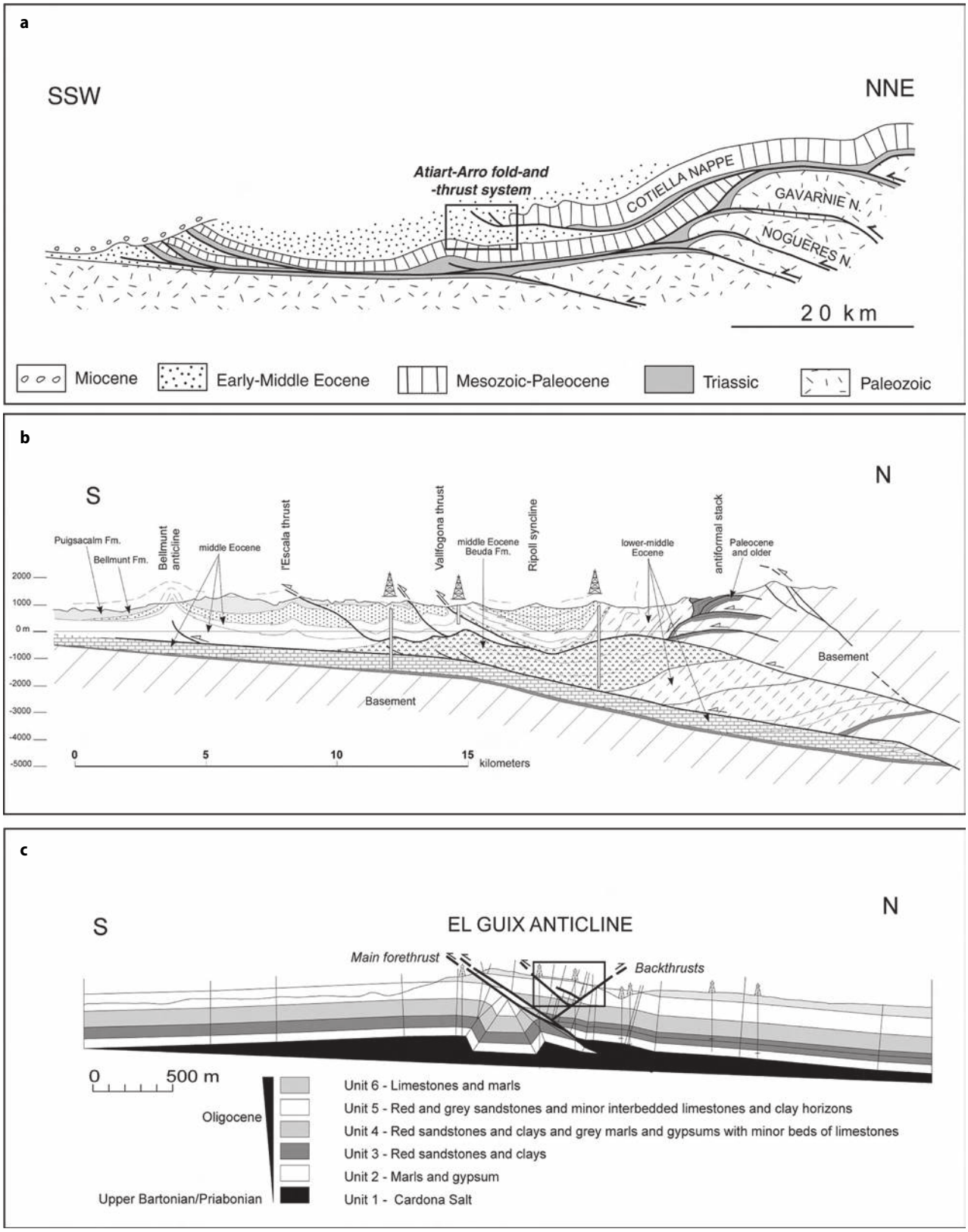


**Fig. 3.** Cross-sections of the studied areas. **a**) Atiart-Arro fold-and-thrust system (schematic section before erosion of the inner part of the Cotiella nappe). The box corresponds to Fig. 4. **b**) L'Escala thrust. **c**) El Guix anticline. The box corresponds to Fig. 8

## 3 Early Development of Submarine Thrust Front: Atiart-Arro Fold-and-Thrust System

### 3.1 Geological Framework

The Atiart-Arro fold-and-thrust system is located in the eastern part of the Ainsa sub-basin, a marine depocentre in the inner part of the central South-Pyrenean basin. The Ainsa sub-basin is mainly filled up by lower and middle Eocene marls with sandstone and conglomerate intercalations forming turbiditic channel-levee complexes, and comprises westward prograding outer-shelf/slope facies intercalations in the eastern part (e.g. Mutti et al., 1988). Th se deposits rest above Upper Cretaceous-Paleocene shelf carbonates, Permo-Triassic marls and sandstones, and a Paleozoic basement. The northern part of the basin-fill is thrust by the Cotiella Nappe, detached in the Triassic sediments and mainly consisting of Upper Cretaceous-Paleocene carbonates (Fig. 4) (Séguret, 1972). The nappe moved southwards for at least 20 km and was probably rooted in the Paleozoic basement of the Axial Zone of the belt, although this root cannot be precisely identifi d due to subsequent deformation and erosion (e.g. Martinez-Peña & Casas-Sainz, 2003). The Atiart-Arro fold-and-thrust system is a SW-verging imbricate structure developed in the basin-fill at the front of the nappe. Erosional surfaces and unconformities related to the fold-and-thrust system show that the main movement of the Cotiella Nappe occurred during the early Eocene (Ypresian), and that deformation continued during the middle Eocene (Mutti et al., 1988).

The study of the fluid behaviour was carried out on four hectometric-scale outcrops, corresponding to three thrust-fault zones and one syncline: the Sampert, Atiart, and Los Molinos thrusts, from the NE to the SW (and structurally from top to bottom), and the Arro syncline in the footwall of the Los Molinos thrust (Fig. 4) (Travé et al., 1998). The Atiart and Los Molinos thrusts probably root within the Cotiella thrust, whereas the Samper thrust is a rootless "out-of-the-syncline" thrust. The Arro syncline is asymmetric, with a steeply-dipping eastern limb and a gently-dipping western limb.

The studied mesostructures aff ct mainly marly lithologies. The thrust fault zones consist in a-few-metres thick intervals where deformation is marked by the association of shear bands in marls and calcite shear veins. Calcite veins are also observed over a few tens of metres in the thrust-fault footwalls, but they are rare or absent in the hangingwalls. The shear bands feature S-C structures related to the development of pressure-solution cleavage. The most intensely strained shear bands have mineral assemblages characterised by the occurrence of dickite, which is absent in the protolith as well as in the less strained domains of fault zones (Buatier et al., 1997). Many calcite veins show a three-stage evolution of their microstructure with 1) diffuse veinlet networks associated with sand disaggregation, 2) crack-seal shear microstructures forming most of the vein volume, and 3) late extensional openings. The geometry of stage 1 and 2 microstructures is coherent with the syn-thrust shearing kinematics and their

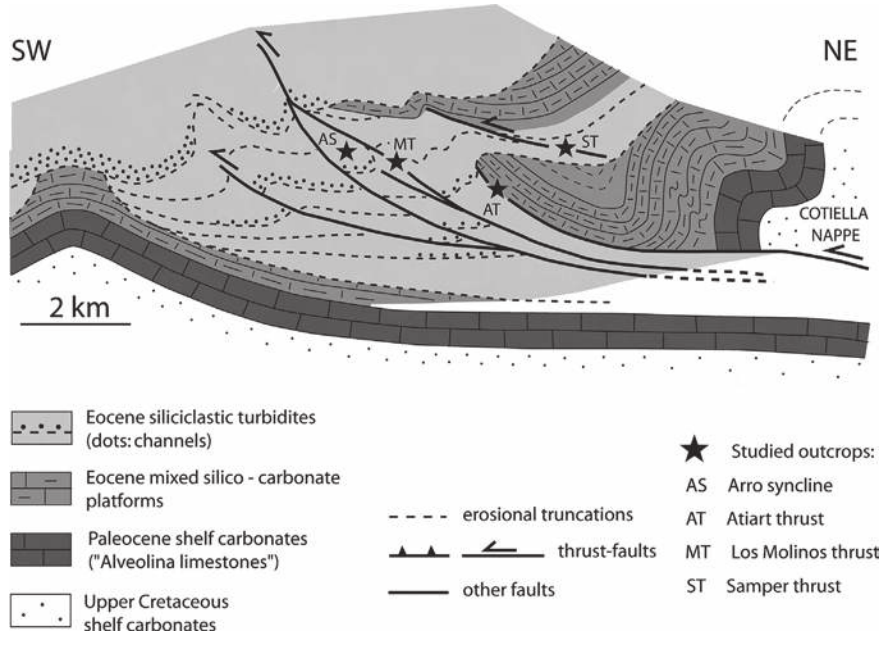


**Fig. 4.** Detailed cross-section of the Atiart-Arro fold-and-thrust system.

chronology relates to the progressive induration of the sediment during vein formation, whereas stage 3 corresponds to a syn- or post-shear boudinage of the veins forming tabular bodies more competent than the surrounding marls. The crack-seal microstructures attest the episodic nature of fault slip and calcite precipitation. Similar shear veins are also present in the Arro syncline, with three generations that formed before, during and after folding, respectively. The most-abundant ones are the syn-folding veins, which formed along the bedding planes in relation to bedding-slip in the steep limb of the syncline. In the Arro syncline, as well as in the Samper and Los Molinos thrusts, calcite veins contain minor amounts of celestite. Other petrographic features of the veins are described in Travé et al., (1997).

Macroscopic deformation is weak outside the thrust fault zones and regional cleavage is absent. However, a locality in the western limb of the Arro syncline features oval burrows that attest about 20% of NE-SW horizontal shortening prior to sediment lithification (Travé et al., 1998). Sand disaggregation observed in the earliest stages of shear vein formation also shows that deformation aff cted initially poorly-lithifi d sediments.

### 3.2 $\delta^{18}O$ and $\delta^{13}C$ of Host Rock and Calcite Veins

The $\delta^{18}O$ and $\delta^{13}C$ values from the host marls range from -8.2‰ to -5.8‰, and from -3.3 ‰ to -0.7‰ PDB, respectively (Fig. 5, Table 1). Th y are thus lower than those of the Eocene marine carbonates which range from -4‰ to +2‰ and from -0.3‰ to +2.8‰ PDB, respectively (Shackleton & Kennett, 1975; Veizer & Hoefs, 1976; Hudson & Anderson, 1989), this depletion most probably resulting from burial diagenesis.

Calcite cements from the three microscopic stages of vein development, as well as the pre-, syn- and post-syncline veins at Arro do not show significant diff rences of isotopic values. On each outcrop, the oxygen isotopic values of the calcite cements in veins are systematically depleted between 1.3 and 2.8‰ PDB in relation to the host marl calcite, probably indicating a higher temperature of the fluid from which the vein calcite precipitated with respect to its adjacent host rock (Marshall, 1992), or a deeper setting of precipitation.

The Atiart and Los Molinos thrusts, which are deep-rooted thrusts, also show depletion in $^{13}C$ of the calcite in veins with respect to the host marl calcite. This is interpreted as an input of an external $^{13}C$-depleted mineralising fluid channelized through the thrust-fault zones. On the contrary, in the Arro syncline and the Samper thrust, which have no roots towards deeper domains, the similar $\delta^{13}C$ in the calcite from veins and host marls shows that the $\delta^{13}C$ of the mineralising fluid was mainly controlled by that of the host sediment.

The isotopic values of calcite from the dickite-bearing marls in thrust zones range from -9.0‰ to -5.8‰ PDB in $\delta^{18}O$, and from -2.6‰ to -1.5 ‰ PDB in $\delta^{13}C$, respectively, i.e. without significant diff rences with respect to calcite from the less deformed marls. However, the calcite veinlets inside these dickite-bearing marls show higher $\delta^{18}O$ values (from -7.3‰ to -4.4‰ PDB in $\delta^{18}O$, and from -2.5‰ to -1.6‰ PDB in $\delta^{13}C$), probably resulting from in situ clay-water reactions, i.e. the dickite formation through partial dissolution of illite and drainage of potassium by fluid flow

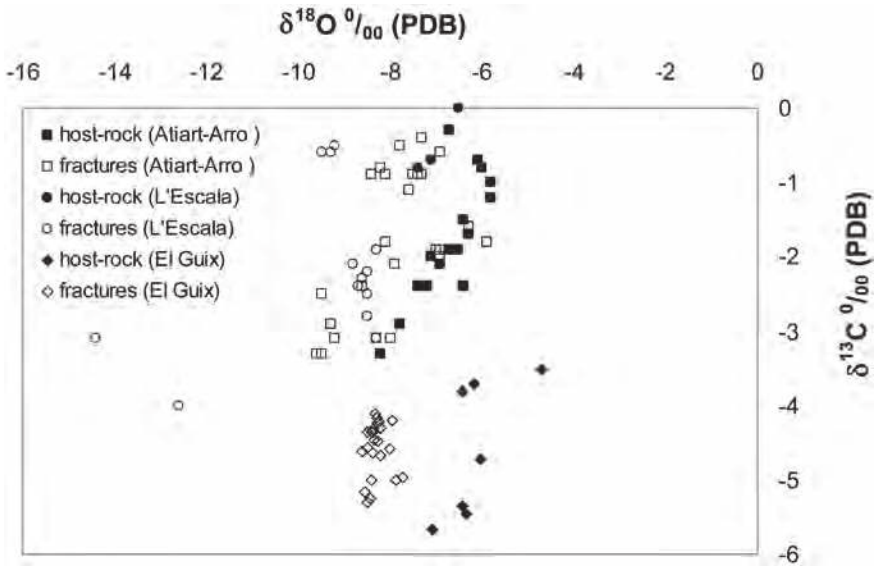


**Fig. 5.** $\delta^{18}O$ versus $\delta^{13}C$ of calcite cements in the veins and host-rocks.

**Table 1.** $\delta^{18}O$, $\delta^{13}C$ and $^{87}Sr/^{86}Sr$ ratio of calcite cements in the veins and host-rocks. The column dif $\delta^{18}O$ indicates the difference between de $\delta^{18}O$ of the calcite cement in the veins and its adjacent host-rock. For Atiart-Arro and El Guix, G1, G2 and G3 refer to the three stages of microstructure development, respectively.

| Structure/ microstructure | | | | $\delta^{18}O$ | $\delta^{13}C$ | dif $\delta^{18}O$ | $^{87}Sr/^{86}Sr$ |
|---|---|---|---|---|---|---|---|
| Atiart-Arro | Thrusts | Atiart thrust | G 2 | -7.8 | -0.5 | 1.7 | |
| | | | G 2 | -8.1 | -1.8 | 2.0 | |
| | | | G 2 | -6.9 | -0.6 | 0.8 | |
| | | | G 2 | -7.5 | -0.9 | 1.4 | |
| | | | Host-rock | -6.1 | -0.7 | | 0.707914 |
| | | Syncline Arro | G 2 | -8.2 | -0.8 | 1.5 | |
| | | | G 2 | -8.2 | -0.8 | 1.5 | |
| | | | G 2 | -7.3 | -0.9 | 0.6 | |
| | | | G 2 | -8.4 | -0.9 | 1.7 | |
| | | | Host-rock | -6.7 | -0.3 | | |
| | | | Host-rock | -5.8 | -1 | | 0.707892 |
| | | | Host-rock | -5.8 | -1.2 | | |
| | | | Host-rock | -5.8 | -1.2 | | |
| | | | G 2 | -8.1 | -0.9 | 2.3 | 0.707862 |
| | | | G 3 | -7.6 | -1.1 | 2.6 | 0.707912 |
| | | | G 1 | -7.3 | -0.4 | 1.5 | 0.707886 |
| | | | G 2 | -7.4 | -0.9 | 1.4 | 0.707916 |
| | | Los Molinos | G 2 | -9.2 | -3.1 | 1.8 | 0.709173 |
| | | | Host-rock | -7.4 | -2.4 | | |
| | | | G 2 | -9.6 | -3.3 | 2.2 | |
| | | | Host-rock | -6.4 | -2.4 | | |
| | | | Host-rock | -6.9 | -2.1 | | |
| | | | Host-rock | -6.7 | -1.9 | | |
| | | Samper | G 2 | -9.5 | -3.3 | 2.3 | |
| | | | Host-rock | -7.2 | -2.4 | | |
| | | | Host-rock | -6.5 | -1.9 | | |
| | | | Host-rock | -6.4 | -1.5 | | |
| | | | G 2 | -5.9 | -1.8 | 0.5 | 0.708153 |
| | | | G 2 | -6.9 | -2 | 0.5 | |
| | | | G 2 | -7 | -1.9 | 0.6 | |
| | | | G 2 | -6.9 | -1.9 | 0.5 | |
| | | | G 2 | -7.9 | -2.1 | 1.5 | 0.708247 |
| | | | Host-rock | -7.1 | -2 | | |
| | | | Host-rock | -6.3 | -1.7 | | |
| | | | Host-rock | -6 | -0.8 | | |
| | | | G 2 | -6.3 | -1.6 | 0.3 | |
| | | | Host-rock | -8.2 | -3.3 | | |
| | | | Host-rock | -7.8 | -2.9 | | |
| | | | G 2 | -9.3 | -2.9 | 1.1 | |
| | | | G 2 | -9.5 | -2.5 | 1.3 | |
| | | | G 2 | -8.3 | -3.1 | 0.5 | |
| | | | G 2 | -9.2 | -3.1 | 1 | |
| | | | G 2 | -8.6 | -2.4 | 0.4 | |
| | | | G 2 | -8 | -3.1 | 0.2 | |

| Structure/ microstructure | | | | $\delta^{18}O$ | $\delta^{13}C$ | dif $\delta^{18}O$ | $^{87}Sr/^{86}Sr$ |
|---|---|---|---|---|---|---|---|
| L'Escala | pre-thrust | | pre-thrust diaclase | -8.5 | -2.8 | 1.1 | 0.708179 |
| | | | pre-thrust diaclase | -8.3 | -1.9 | 0.9 | |
| | thrust | | bed to bed sliding | -8.8 | -2.1 | 1.4 | |
| | | | thrust fault | -8.3 | -3.1 | 0.9 | 0.708165 |
| | | | thrust fault | -8.6 | -2.3 | 1.2 | |
| | | | thrust fault | -8.5 | -2.2 | 1.1 | 0.708171 |
| | | | bed to bed sliding | -8.5 | -2.5 | 1.1 | 0.708189 |
| | | | bed to bed sliding | -8.7 | -2.4 | 1.3 | |
| | | | sinistral fault | -9.5 | -0.6 | 2.1 | |
| | post-thrust | | Host-rock | -6.5 | 0 | | |
| | | | NW-SE diaclase | -12.6 | -4 | 5.2 | |
| | | | Host-rock | -7.4 | -0.8 | | |
| | | | NW-SE diaclase | -14.4 | -3.1 | 7.3 | 0.70847 |
| | | | Host-rock | -7.1 | -0.7 | | 0.708952 |
| | | | sinistral fault | -9.2 | -0.5 | 2.5 | 0.708572 |
| | | | Host-rock | -6.7 | -0.3 | | |
| | | | sinistral fault | -9.3 | -0.6 | 2.6 | |
| El Guix | less deformed area | | Host-rock | -6.34 | -5.46 | - | 0.70941 |
| | | | Host-rock | -6.42 | -5.35 | - | |
| | | | G 2 | -7.88 | -5.01 | 1.5 | 0.70911 |
| | | | G 2 | -7.72 | -4.97 | 1.3 | 0.70911 |
| | | | G 2 | -8.41 | -5.01 | 2.0 | |
| | | | G 2 | -8.56 | -5.16 | 1.5 | |
| | | | G 2 | -8.49 | -5.3 | 1.4 | |
| | | | G 2 | -8.44 | -5.24 | 1.4 | |
| | | | Host-rock | -7.07 | -5.66 | - | |
| | fore-thrust | | G 2 | -8.49 | -4.57 | 3.8 | 0.70887 |
| | | | G 2 | -8.61 | -4.61 | 3.9 | |
| | | | Host-rock | -4.7 | -3.52 | - | 0.70865 |
| | lower backthrust | | G 1 | -8.5 | -4.36 | 2.5 | |
| | | | G 2 | -8.2 | -4.3 | 2.2 | 0.70909 |
| | | | G 2 | -8.42 | -4.36 | 2.4 | 0.70909 |
| | | | G 2 | -8.37 | -4.36 | 2.4 | 0.70909 |
| | | | G 2 | -8.38 | -4.32 | 2.4 | 0.70909 |
| | | | G 2 | -8.34 | -4.46 | 2.3 | |
| | | | G 2 | -8.28 | -4.47 | 2.3 | |
| | | | Host-rock | -6.02 | -4.72 | | |
| | upper backthrust | | G 2 | -8.01 | -4.58 | 1.9 | 0.70906 |
| | | | G 3 | -8.28 | -4.23 | 2.1 | |
| | | | G 2 | -8.32 | -4.11 | 2.3 | 0.70906 |
| | | | Host-rock | -6.16 | -3.71 | | 0.70878 |
| | | | G 2 | -8.37 | -4.63 | 2.0 | |
| | | | G 2 | -8.22 | -4.67 | 1.8 | |
| | | | Host-rock | -6.42 | -3.82 | | |
| | up.b.foo. | | G 2 | -8.31 | -4.17 | 1.9 | |
| | | | G 2 | -7.97 | -4.2 | 1.6 | |
| | | | G 2 | -8.25 | -4.21 | 1.8 | |

along the shear zones (Buatier et al., 1997). Alteration of rock-fragments and feldspars has been proved to produce an $^{18}O$ increase in the fluid (Yeh & Savin, 1977; Longstaff , 1993). In the context of the Atiart-Arro thrust system, the kinematics of dickite formation are inferred to have been promoted by strain and fluid flow (Buatier et al., 1997), rather than by temperature as classically described in diagenetic or hydrothermal environments. Comparing the values of the four outcrops, both the host marl calcite and the calcite cements in veins show a progressive depletion in both $^{18}O$ and $^{13}C$ from the Atiart thrust and Arro syncline to Los Molinos thrust and to the Samper thrust (Travé et al., 1997). The structural location and burial history of the four outcrops make it difficult to explain the trend of isotopic depletion by diff rences in burial of the structures. A possible explanation could be a higher meteoric influence in the structures located closer to the emerged part of the belt (i.e. the Samper thrust).

### 3.3 $^{87}Sr/^{86}Sr$ Values of Host Rock and Veins

In the Arro syncline, the calcite and celestite veins and the calcite fraction of the host marls, show $^{87}Sr/^{86}Sr$ ratio ranging between 0.70774 and 0.70795, without a significant diff rence between the pre-, syn- and post-syncline veins (Fig. 6, Table 1). This range of values is consistent with the $^{87}Sr/^{86}Sr$ ratio of the Eocene seawater (Katz et al., 1972; Burke et al., 1982; DePaolo & Ingram, 1985), indicating that the source of strontium to precipitate the calcite and celestite in veins and the calcite cement in the host sediment was the same. The later was controlled by the $^{87}Sr/^{86}Sr$ ratio of the Eocene seawater during the whole evolution of the Arro syncline. The $^{34}S$ values of the celestite also indicates precipitation from an Eocene marine water (Travé et al., 1997). Th refore, the vein-forming fluid was probably the interstitial water trapped in the Eocene marine marls derived from the Eocene seawater, or a fluid equilibrated with the Eocene calcitic sediments.

The siliciclastic detrital fraction in the marls has substantially higher $^{87}Sr/^{86}Sr$ ratios (0.71723–0.71894) with respect to the Eocene seawater, giving rise to the more radiogenic $^{87}Sr/^{86}Sr$ ratios in the bulk marl (0.70976–0.70987) than in the calcite fraction. This indicates that this detrital fraction originates from the erosion of Paleozoic rocks outcropping in the paleo-Axial Zone.

In the Atiart and Los Molinos thrust-fault zones, the $^{87}Sr/^{86}Sr$ ratios in vein calcite range from 0.70815 to 0.70927, i.e. more radiogenic than the Eocene seawater values. Th se relatively high values indicate that the vein calcite in fault zones precipitated from a fluid with a diff rent composition than the fluid present outside the fault zones and, consequently, that these zones acted as fluid conduits during shear deformation. This more radiogenic fluid composition could originate from 1) interaction with the Paleozoic rocks or the Eocene marls existing in deeper settings, 2) in-situ mineralogical transformations of the Eocene marls in the intensely strained sediments (e.g. the illite to dickite transformation), or 3) the weathering by meteoric water of the Paleozoic rocks in the emerged part of the belt. In the case that the source was the Eocene marls, either from deeper settings or from local more deformed part of the thrust-fault zones, the detrital phyllosilicates submitted to higher temperature and/or pressure could have expelled their more radiogenic Sr during dissolution and mineralogical transformations. The three sources are possible and they could have acted alone or simultaneously.

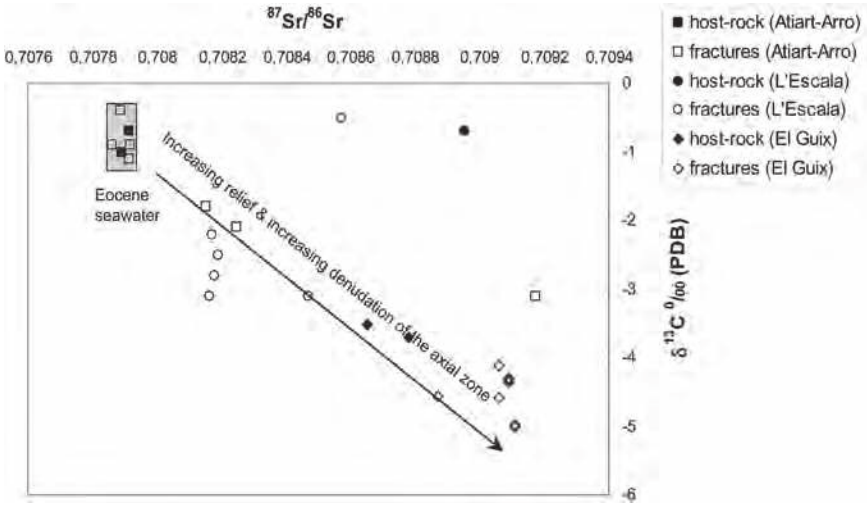


**Fig. 6.** $^{87}Sr/^{86}Sr$ ratio versus $\delta^{13}C$ values of calcite cements in the veins and host-rocks.

### 3.4 Elemental Geochemistry

The elemental composition of the fluid from which calcite precipitated was determined from the elemental geochemistry of the calcite cements (Travé et al., 1997). The results show that the elemental composition of the fluid from which all types of calcite precipitated had a Mg/Ca ratio between 0.006 and 0.126, a Sr/Ca ratio between 0.012 and 0.39, a Mg/Sr ratio between 0.089 and 4.938, a Ca/Fe ratio between 79 and 8286, and a Mn/Ca ratio between $0.1 \times 10^{-4}$ and $4 \times 10^{-4}$. Most of these values are consistent with formation water and not with unmodifi d marine waters or oxidizing/reducing meteoric waters. The samples from the Atiart thrust and Arro syncline have higher values of Sr/Ca and lower values of Mg/Sr than the samples from the other two outcrops, reflecting original seawater composition to a certain extent (Travé et al., 1997).

### 3.5 Fluid Circulation in the Early Development of the Submarine Thrust Front

Syn-kinematic fluid flow in the submarine thrust front during the early-middle Eocene is evidenced macroscopically by the abundance of calcite shear veins within the marls involved in the Atiart-Arro fold-and-thrust system.

Microstructures indicate that deformation aff cted initially poorly lithifi d sediment, and the crack-seal mechanism of formation of the shear veins attests the episodic nature of fault-slip and associated fluid flow in fractures. Distribution of the veins suggests that the main source of fluid was dewatering of the poorly permeable marls from the thrust footwalls, probably related to both (i) vertical compaction due to burial under thrust sheets, and (ii) tectonic horizontal shortening. Th se fluids were drained upwards towards the thrust-fault zones, in which they migrated laterally towards the thrust front due to the anisotropy of the fracture permeability in these zones.

The $^{87}Sr/^{86}Sr$ ratios of the host marl calcite and of the calcite and celestite in the veins away from the thrust-fault zones indicate that the original water trapped interstitially in the marls was Eocene seawater. This is corroborated by the $\delta^{34}S$ in the vein celestite from the Arro syncline, which yielded values ranging from 18.3 to 21.7‰ (CDT) (Travé et al., 1997), consistent with those of the Eocene seawater sulphate (Claypool et al., 1980). The $\delta^{18}O$ and $\delta^{13}C$ values of the same samples reveal a change of the porewater composition from marine to formation-water during the early burial stage. Fluid inclusion microthermometry of the celestite in the Arro syncline veins, indicating homogenization temperatures ranging between 157 and 183°C and salinities around 7 wt% eq. NaCl (Travé et al., 1998), reveal the presence of a hot, saline ascending fluid restricted to the veins, where it was mixed with the local formation water (Travé et al., 1998). Th se two types of fluids were drained towards the thrust-fault zones where they acquired a higher $^{87}Sr/^{86}Sr$ ratio, probably related to local fluid-sediment reactions (the dickite formation). The $\delta^{13}C$ depletion in vein calcite from the Atiart and Los Molinos thrusts may result from the input along the thrust zones of $^{13}C$-depleted mineralising fluids, whereas the $\delta^{18}O$ depletion in the calcite from the structurally highest/innermost thrust-fault zones suggests also the influence of meteoric water derived from the emerged part of the belt in these structures.

The earliest fluid regime in the Ainsa basin was an intergranular (porous) flow of the local fluid (compactional flow) allowing for a pervasive isotopic and elemental exchange with the marls prior to vein formation. With the onset of compressional deformation, channelized flow along tectonic slip surfaces became dominant, contributing to local sediment dewatering, but also to the input of external fluids along the thrust fault zones. The geochemical data do not record significant evolution of fluid composition during the successive episodes of vein formation along the slip surfaces at a same locality. Such a fluid regime dominated by the dewatering of local sediments is consistent with the submarine context of deformation that aff cted recently deposited, poorly lithifi d sediments. This tectonic context suggests that fluids may have been overpressured.

## 4 Intermediate Development of the Fold-and-Thrust System within a Marine-Continental Transitional Environment: L'Escala Thrust

### 4.1 Geological Framework

The L'Escala thrust is part of the Alpens-L'Escala antiformal structure within the south-eastern Pyrenean foreland basin (eastern Catalan basin) (Muñoz et al., 1986). The structure is constituted by thrusts and folds aff cting the middle and upper Eocene alluvial fan and deltaic syn-tectonic deposits of the Bellmunt and Puigsacalm Formations, respectively (Fig. 7). The folded foreland is limited at the north by the Vallfogona thrust and, at the south, by the Bellmunt anticline from the subhorizontal sediments of the Ebro basin (Fig. 3b).

The L'Escala anticline developed in the hanging-wall of a thrust which places middle-upper Lutetian continental sediments of the Bellmunt Formation over

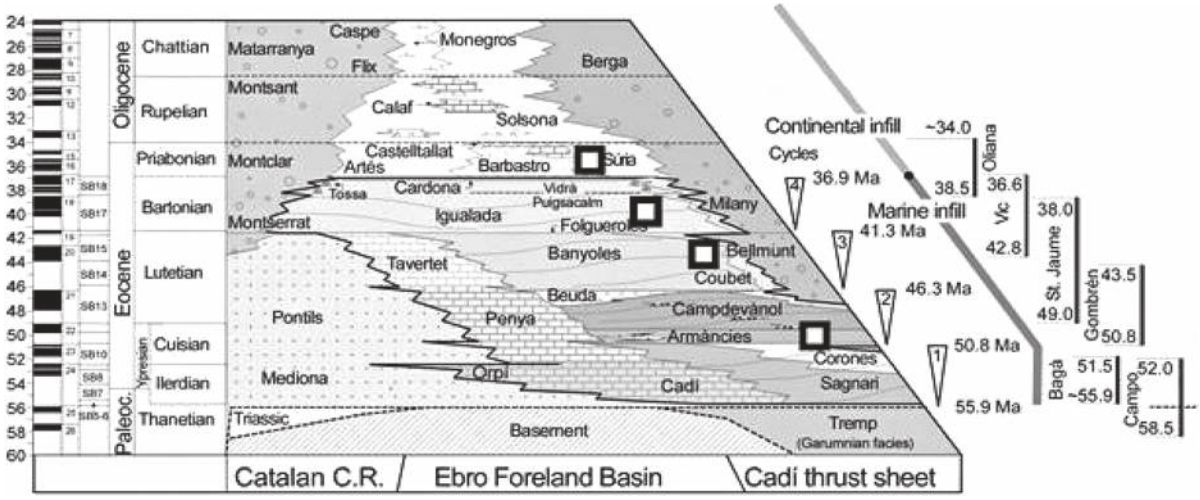


**Fig. 7.** Stratigraphic framework of the south-eastern Pyrenean foreland basin with location of the El Guix outcrop (upper square), L'Escala outcrop (two intermediate squares), and Armancies Formation (lower square).

lower Bartonian marine sediments of the Puigsacalm Formation (Muñoz et al., 1986).

The Bellmunt Formation is constituted by a clastic succession evolving from fluvio-deltaic to alluvial red deposits prograding from the Pyrenean Axial Zone towards the south margin of the Lutetian basin (Ramos et al., 2002). The limit between the Bellmunt Formation and the Puigsacalm Formation is sharp and corresponds to a marine transgression at a basin scale. The Puigsacalm Formation is constituted by grey microconglomerates and sandstones with glauconite prograding from the east and forming metric-thick sequences interpreted as deltaic systems.

In the studied outcrop, the Bellmunt Formation is formed by decimetric to metric intervals of clays, siltites, sandstones, and conglomerates interpreted as channel and flood plain deposits. The Puigsacalm Formation in the studied outcrop basically consists of calcite cemented sandstones.

The sampled section comprises three diff rent thrust fault zones. The main fault places materials of the Bellmunt Formation on top of the Puigsacalm Formation, and the other two faults aff ct only the Bellmunt Formation. Three sets of cross-cut calcite-filled fractures have been recognised: 1) extensional pre-thrust fractures (cut and deformed by the thrust plane), 2) thrust-related shear-fractures (thrust faults and associated bed to bed sliding), and 3) post-thrust fractures cutting the thrust planes. The latter consists of: 3a) sinistral strike-slip faults, and 3b) NW-SE extensional fractures. The pre-thrust fractures have only been observed in the Bellmunt Formation. Calcite cements within the thrust faults have been observed in the three thrust faults and calcite cements in the bedding planes have been only observed in the Bellmunt Formation. Calcite cements in the thrust faults and in the bedding planes precipitated synchronously to thrust activity due to successive shear openings, as indicated by the occurrence of shear bands formed by the crack-seal mechanism. The post-thrust sinistral strike-slip faults and NW-SE fractures have been only observed in the footwall of the lower thrust in the Puigsacalm Formation. The former are filled by calcite cement precipitated synchronously to shear-fault opening, whereas the NW-SE fractures correspond to extensional diaclases, parallel to the compression-related cleavage planes, and filled by calcite cement not aff cted by pressure-solution related to cleavage formation.

The pre-thrust fractures are diaclases with sharp, straight or undulated walls and are filled by calcite cements constituting veins from 1 cm to 5 cm thick and up to several metres long. Th se fractures are filled by two generations of cement: a first generation constituted by a non isopachous rim of euhedral calcite crystals and a second generation of anhedral sparry calcite cement from few millimetres up to 2 centimetres thick, with deformed mechanical twin planes and undulating extinction.

The thrust fractures are the thrust faults and the associated stratification planes which moved synchronously to the thrust movement due to bed to bed sliding and are filled by calcite cements constituting veins from 1 to 10 cm thick. The veins within the thrust fractures are constituted by calcite cement, forming diff rent shear bands (up to 6 successive shear bands have been observed in a single fracture) parallels to the fracture wall. Locally, the limits between the shear bands are stylolitic surfaces. Each shear band is formed by a crack-seal mechanism. The calcite crystals are brown-

ish-greenish, anhedral or subeuhedral, locally elongated, variable in size from 30 μm up to 2 mm, smaller close to the crack-seal border and increasing in size farward. The bigger crystals show abundant mechanical twinning planes and undulating extinction.

The post-thrust fractures include two sets of fractures: the sinistral faults and the NW-SE fractures. The veins filling the sinistral faults are constituted by calcite crystals, with planar or interpenetrated borders. The crystals are transparent and up to 5 mm large and show mechanical twinning planes and undulating extinction. The NW-SE fractures are diaclases. The fracture walls are sharp and straight. The fractures are filled by euhedral sparry transparent calcite crystals up to 5 millimetre large, with planar or interpenetrated borders, abundant deformed mechanical twinning planes and undulating extinction.

## 4.2 $\delta^{18}O$ and $\delta^{13}C$ of Host Rock and Calcite Veins

The $\delta^{18}O$ of the Puigsacalm Formation host rock range from -7.4 to -6.5‰ PDB and the $\delta^{13}C$ range from -0.8 to 0.0‰ PDB (Fig. 5, Table 1). Th se values are more depleted in $\delta^{18}O$ and within the same range for $\delta^{13}C$ than the isotopic values of the Eocene marine carbonates (from -4 to +2‰ PDB and from -0.3 and +2.8‰ PDB, respectively). Th se depleted $\delta^{18}O$ values of the bulk host rock are probably a mixture of depleted $\delta^{18}O$ values of the calcite cement precipitated in the interparticle porosity during relative burial conditions and a more enriched $\delta^{18}O$ values of the marine components. The $\delta^{13}C$ values around 0‰ probably indicate that the main source for C to produce the calcite cements may have been the marine bioclastic components (Discocyclines, Nummulites, echinoderms, bivalvia, bryozoans,..) which form 50% of the Puigsacalm Formation host rock.

The carbonate fraction of the Bellmunt Formation host rock has not been analysed because the texture of the rock did not allow to analyse separately the calcite cement from the abundant Paleozoic, Mesozoic and older Tertiary carbonate clasts.

The $\delta^{18}O$ and the $\delta^{13}C$ values of the calcite cement in the pre-thrust fractures range from -8.5 to -8.3‰ PDB and from -2.8 and -1.9‰ PDB, respectively. The $\delta^{18}O$ and the $\delta^{13}C$ of the calcite cement in fractures related to bed to bed sliding and in the thrust faults are very similar, ranging from -8.8 to -8.3‰ PDB and from -3.1 to -2.1‰ PDB, respectively. The similarity of the $\delta^{18}O$ and $\delta^{13}C$ between the calcite cements within pre-thrust and thrust-related fractures indicates that both precipitated from the same fluid or from diff rent fluids with similar composition, which is less probable. Hence, during thrusting, the pre-thrust fractures became open for fluid circulation and for precipitation of calcite cements.

The $\delta^{18}O$ of the calcite cement in the post-thrust strike-slip faults range from -9.5 to -9.2‰ PDB and the $\delta^{13}C$ range from -0.6 to -0.5‰ PDB. Th se $\delta^{18}O$ values are on average 2-3‰ more depleted than those of the Puigsacalm Formation bulk host rock, whereas the $\delta^{13}C$ values are within the same range as those of the host rock. The similarity between the $\delta^{13}C$ values between the host rock and the calcite cement within the fractures indicates host-rock buff ring. The diff rence in $\delta^{18}O$ between the bulk host rock and the calcite cement within the pre-thrust and thrust-related fractures and post-thrust strike-slip faults, is probably because $\delta^{18}O$ of the bulk host rock is a mixture between a lower $\delta^{18}O$ of the interparticle calcite cement and a $\delta^{18}O$ closer to 0‰ of the marine bioclastic components, whereas the $\delta^{18}O$ of the calcite cements within the fractures reflect only the composition of the calcite cement which has a non marine origin, either precipitated from meteoric or from formation waters.

The $\delta^{18}O$ of the calcite cement in the post-thrust NW-SE fractures range from -14.4 to -12.6‰ PDB and the $\delta^{13}C$ range from -4.0 to -3.1‰ PDB. The $\delta^{18}O$ of the calcite cement in the post-thrust NW-SE fractures is in average 6-7‰ more depleted than the Puigsacalm Formation host rock, and the $\delta^{13}C$ is in average 3-4‰ more depleted than the host rock. The very low $\delta^{18}O$ values suggest a relatively hot fluid. The depleted $\delta^{13}C$ values indicate that this external fluid was probably, in origin, a meteoric fluid enriched in $^{12}C$ probably due to the ingress of isotopically light soil-$CO_2$ (Cerling, 1984; Cerling et al., 1989). This fluid did not interact with the Puigsacalm Formation host rock.

## 4.3 $^{87}Sr/^{86}Sr$ Values of Host Rock and Calcite Veins

The $^{87}Sr/^{86}Sr$ ratio of the Puigsacalm Formation bulk host rock is 0.70895. In the calcite cements, values are 0.70818 in the pre-thrust fractures, 0.70816 to 0.70817 in the thrust fault zones, 0.70819 in the bedding-parallel veins, 0.70857 in the post-thrust strike-slip faults, and 0.70847 in the post-thrust NW-SE fractures (Fig. 6, Table 1).

The $^{87}Sr/^{86}Sr$ ratio of the Bartonian sea (age of the Puigsacalm Formation) was 0.7077–0.7078 (DePaolo & Ingram, 1985; Hess et al., 1986; Koepnick et al., 1985; Mead & Hodell, 1995; Palmer & Elderfi ld, 1985) and, therefore, all the studied cements are non marine in origin.

The $^{87}Sr/^{86}Sr$ ratio of the Puigsacalm Formation bulk host rock (0.70895) reflects the mixture of the bioclastic Eocene marine components and the silici-

clastic fraction derived from an external source, probably the interaction of fluids with Paleozoic rocks.

The $^{87}Sr/^{86}Sr$ ratio homogeneity of calcite cements in the pre-thrust fractures, thrust fault zones and bedding-parallel veins, indicates a common origin for the fluid, as already suggested by the oxygen and carbon isotopic values. This radiogenic fluid composition could originate from 1) interaction with the Paleozoic rocks or the Paleozoic siliciclastic components of the Puigsacalm Formation host rock existing in deeper settings, 2) in-situ mineralogical transformations of the Paleozoic siliciclastic components of the host rock, or 3) the weathering by meteoric water of the Paleozoic rocks in the emerged part of the belt.

The calcite cements in the post-thrust strike-slip faults and in the post-thrust NW-SE fractures show $^{87}Sr/^{86}Sr$ values closer to the Puigsacalm Formation host rock values than the cements in the former fractures indicating a higher contribution either of the Paleozoic rocks or of the Paleozoic siliciclastic components of the host rock. In the case of the post-thrust strike-slip faults, the similar $\delta^{13}C$ values are more in agreement with a high contribution of the Paleozoic siliciclastic components of the host rock, whereas in case of the post-thrust NW-SE fractures the lower $\delta^{18}O$ and lower $\delta^{13}C$ of the calcite cement better account for an origin of the $^{87}Sr/^{86}Sr$ values by mineralogical transformations of the underlying Paleozoic rocks, at higher temperature.

## 4.4 Elemental Geochemistry

The calcite veins filling the pre-thrust and thrust-related fractures show a similar range of values characterised by low Fe (between 405 and 2770 ppm), low Sr values (from below the detection limit up to 1735 ppm of Sr), Mn content from 370 up to 1815 ppm, and Mg content between 645 and 7945 ppm.

The calcite veins filling the post-thrust strike-slip faults are characterised by a very high Fe content (between 2915 and 9105 ppm), between 365 and 1260 ppm of Mn, between 885 and 5715 ppm of Mg and from below the detection limit up to 1515 ppm of Sr.

The calcite veins filling the post-thrust NW-SE fractures are characterised by very high Sr content (from 655 and 3535 ppm), between 345 and 1185 ppm of Mn, between 400 and 3195 ppm of Fe, and from below the detection limit up to 1795 ppm of Mg.

The calcite cement filling the porosity within the Puigsacalm Formation host rock has a composition similar to the post-thrust strike-slip faults, with Mn content between 265 and 705 ppm, Fe content between 2595 and 6900 ppm, Mg content between 1230 and 3605 ppm and from below the detection limit up to 445 ppm of Sr.

The cement in the pre-thrust and thrust-related fractures precipitated from a fluid consistent with a meteoric water composition.

The cement in the Puigsacalm Formation host rock and in the post-thrust strike-slip faults precipitated from a fluid consistent with a formation water composition, probably because a deeper burial location of the structure after the thrust emplacement.

The cement in the NW-SE fractures precipitated from a fluid consistent either with a meteoric modifi d to a formation water composition.

## 4.5 Fluid Circulation During the Intermediate Development of the Fold-and-Thrust System within a Marine-Continental Transition Environment

The diff rent stages of vein formations, characterised by diff rent geochemical signatures, attest the evolution of the fluid system during the tectonic history.

### 4.5.1 Prior to the Main Tectonic Shortening

No evidences of fluid circulation exist during the development of the pre-thrust fractures because no precipitation of cement took place. Precipitation of calcite cements within these fractures did not occurred until the main tectonic shortening.

### 4.5.2 The Main Thrust Event

Compressive deformation and thrust emplacement occurred while sedimentation was still active in the basin. The veins related to the main tectonic shortening occur either in the thrust faults or related to bedding slip during flexural folding. The concentration of veins inside and in the few tens of metres below and above the thrust faults and their absence far from the thrust faults indicates that these zones were zones of preferential fluid flow during compressive deformation. As it also occurred in the Ainsa area, the crack-seal mechanism of formation of the calcite shear veins indicates synchronicity between vein formation and fault movement within the thrust-related fractures and attests the episodic nature of fault-slip and associated fluid flow.

A meteoric fluid, with relatively low Fe, low Sr and high Mg content, $\delta^{18}O$ ranging from -8.8 to -8.3‰ PDB and $\delta^{13}C$ ranging from -3.1 to -2.1‰ PDB, and $^{87}Sr/^{86}Sr$ ranging from 0.70816 to 0.70819, circulated through the thrust-related fractures as well as through the pre-thrust fractures during thrust development. This fluid had no or very low interaction with the host

rock. The identical chemical composition of the calcite cement filling the three main thrust faults, the bedding planes and the previously formed fractures indicates that they belonged to the same interconnected fluid system and therefore, the presence of a widespread distributed homogeneous fluid.

The meteoric fluids, derived from the emerged part of the belt and arriving to the thrust fault zones, flowed preferentially along these zones, in a drainage pattern dominated by higher fracture permeability parallel to the thrust faults. Due to this lateral drainage, the thrust fault zones probably acted as barriers hindering their flowing towards more external parts of the belt.

The diff rences in the $^{87}Sr/^{86}Sr$ ratio and $\delta^{13}C$ between the calcite cement in the pre-thrust and thrust-related fractures and the Puigsacalm Formation host rock indicates that the geochemistry of cement was poorly controlled by that of the host rock and, therefore, that the fluid was not buff red by the host rock and an open palaeohydrological system during the main thrust event.

#### 4.5.3 The Post-Thrust Strike-Slip Event

Calcite shear veins precipitated synchronously to strike-slip fault activity following thrusting. The elemental geochemistry of the calcite cements in these faults is consistent with precipitation from a fluid with a formation water composition. The calcite cements precipitated from this fluid are characterised by very high Fe content, $\delta^{18}O$ ranging from -9.5 to -9.2‰ PDB, $\delta^{13}C$ ranging from -0.6 to -0.5‰ PDB and $^{87}Sr/^{86}Sr$ of 0.70857. Th se $^{87}Sr/^{86}Sr$ ratio and $\delta^{13}C$ values are closer to the Puigsacalm Formation bulk host rock values than the calcite cements in all the other fractures indicating the higher intensity of fluid-rock interaction. A high interaction between the fluid and the host rock seems to be restricted, in the studied section, at this episode of the geodynamic evolution, and cementation of the Puigsacalm Formation host rock probably occurred at this time. The $\delta^{18}O$ values of the Puigsacalm Formation bulk host rock probably indicate a mixture between the marine contribution of the bioclastic components and a more depleted contribution of the calcite cement precipitated during burial conditions. The $\delta^{13}C$ values indicate that the main source for carbon to produce the calcite cements may have been the marine bioclastic components which form 50% of the host rock. The $^{87}Sr/^{86}Sr$ ratio indicates the non marine origin of the fluid trapped in the sediment, and the great influence of the siliciclastic components of the host rock. The $^{87}Sr/^{86}Sr$ anomaly in the calcite cement in the fault probably results from local clay mineral reactions.

#### 4.5.4 The Late Extensional Tectonic Phase

The post-thrust NW-SE extensional fractures are the latest observed features, formed by the opening of the pre-existing cleavage planes. Th y thus post-date the compressional deformation.

The calcite cements in these NW-SE fractures, with relatively low Mg and Fe and relatively high Sr content, low $\delta^{18}O$ values ranging from -14.4 to -12.6‰ PDB, $\delta^{13}C$ ranging from -4.0 to -3.1‰ PDB and $^{87}Sr/^{86}Sr$ ratio of 0.70847, are interpreted as precipitated from a hot meteoric fluid. This fluid had no or very low interaction with the carbonate fraction of the Puigsacalm Formation host rock, whereas the $^{87}Sr/^{86}Sr$ ratio indicates contribution of the Palaeozoic rocks. The high temperature during calcite precipitation indicates a deep-circulating fluid.

Thus, at this stage, the paleohydrogeological system remained open to external meteoric fluids arriving from more internal and emerged parts of the belt, but with rather long circulation in relatively deep structures.

The extensional character of these fractures is interpreted as a stage of compressive stress relaxation associated with tectonic uplift nd relief formation.

## 5 Late Development of Continental Thrust and Fold system: El Guix Anticline

### 5.1 Geological Framework

The El Guix anticline corresponds to the southernmost structure of the south-eastern Pyrenean foreland basin, detached above the Priabonian Cardona salt separating the non-deformed strata from the folded and thrusted strata. Compressional activity in the area represents the latest stages of the Alpine compressional tectonics (Sans & Vergés, 1995).

The El Guix anticline is a double structure composed of two anticlines (Fig. 3c). The sampled section displays two sets of linked fractures rooted at diff rent depths and aff cting diff rent lithologies. Structurally, it is located in the northern anticline in which a major north-directed thrust (backthrust) merges with several south-directed thrusts (forethrusts) (Fig. 8). Shortening across the anticline is approximately 21%, consisting of 16% of layer-parallel shortening prior to folding and thrusting, and only 5% during folding and thrusting (Sans et al., 2003).

The deformed sedimentary pile is made up of fine-grained, fluvio-lacustrine deposits, consisting of clays, sandstones and limestones of late Eocene-Oligocene age, overlying the evaporite sequence. Th se rocks are located approximately 300 metres above the detach-

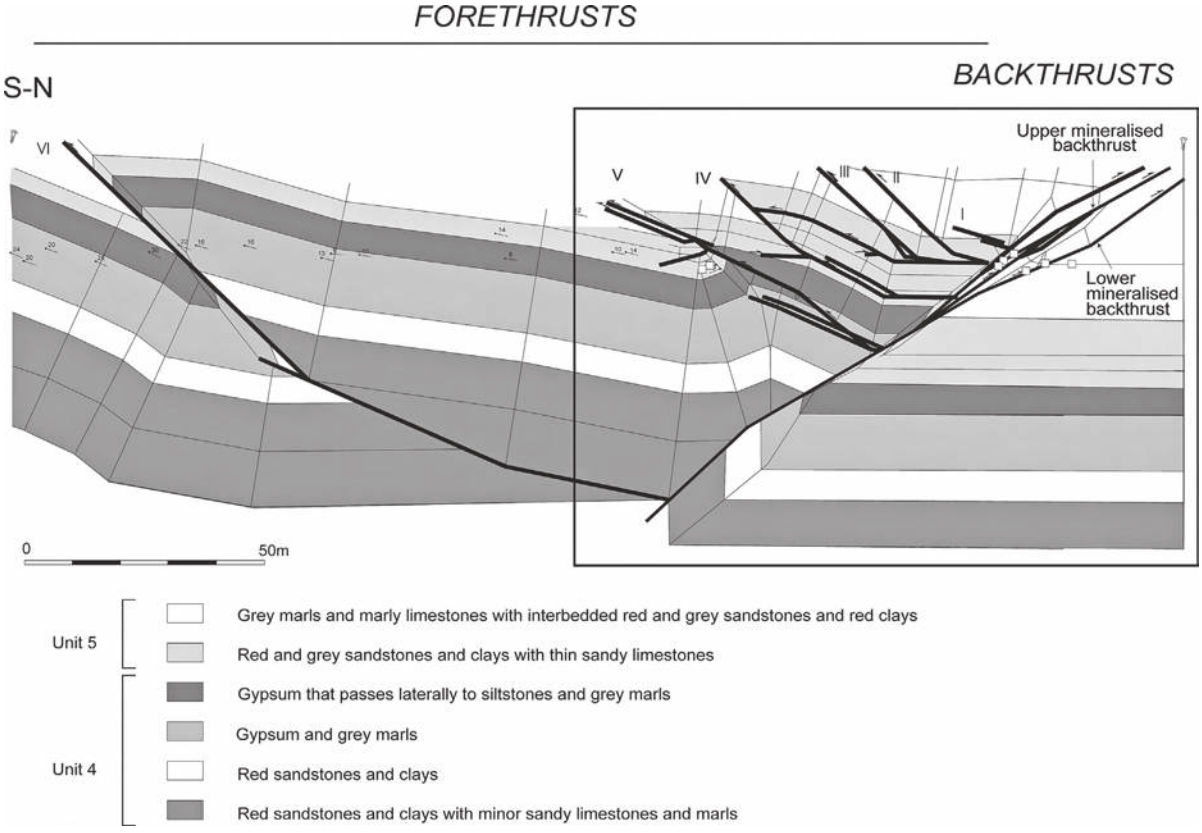


**Fig. 8.** Detail of the sampled structures in the El Guix area.

ment horizon. During thrusting, the maximum burial determined by vitrinite reflectance was 2 km, indicating that the folding and thrusting occurred at depth (Vergés et al., 1998), which is consistent with the pregrowth nature of the deformed rocks.

The backthrust is an intensely deformed, 2 m thick zone, which has an offset of 30 m, formed by an array of four north-directed faults. Only two of them present calcite veins, and they henceforth are refered as lower and upper mineralised backthrust. The footwall of the upper mineralised backthrust presents minor fractures filled with calcite veins. The sediments located between the main forethrust and the backthrust array are deformed by a set of south-directed thrusts (forethrusts) which branch in layer parallel detachments and, at a deeper level, merge with the backthrust (Fig. 8). Forethrusts I to IV only cut sandstone beds, whereas forethrusts V and VI cut sandstone beds and a lower gypsum horizon. None of these forethrusts is mineralised and their slip ranges from half a metre to a few metres. The footwall of forethrust V presents a set of cross-cutting south and north-directed minor faults with an offset of several centimetres. Th se minor faults are filled with calcite veins.

Less deformed areas of the anticline also present small fractures filled with calcite. We studied fractures located about 20 m to the north of the backthrust array aff cting subhorizontal beds of grey marls and fine sandstones, and 200 m above the other samples aff cting horizontal lacustrine limestones in the hangingwall of the backthrust array.

In the El Guix anticline, calcite veins are mostly found where the host rocks are clays and limestones, and are almost absent in the fractures aff cting sandstones. The calcite veins range from millimetres to centimetres in thickness and show slickensides.

The evolution pattern of the calcite-sealed fractures consists of three stages (Fig. 9) which reflect an evolution of the microstructures very similar to that observed at Atiart-Arro. In each fracture, deformation started with a network of discontinuous microfractures (stage 1), slightly oblique to the sedimentary lamination and associated with a ductile deformation of the host sediment. Later, crack-seal shear veins, locally aff cted by micro-stylolitic surfaces, record the main thrust activity (stage 2). Finally, extensional fractures, cross-cut at a large angle the microfractures of stage 2 (stage 3).

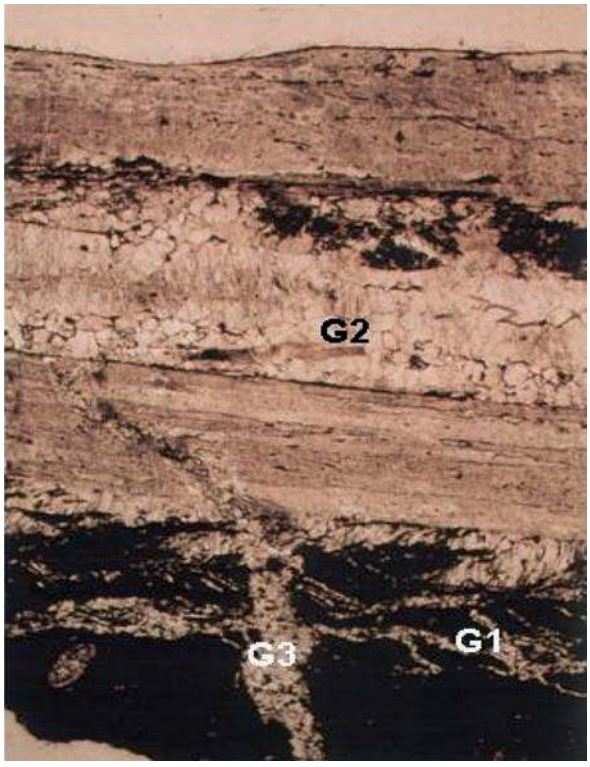


**Fig. 9.** Petrology of the veins showing the three microfracture stages

The cement filling microfracture stage 3 also fills the vuggy porosity aff cting the calcite cement filling microfracture stage 2 and the intergranular porosity of the host rock.

Further petrographic features of the veins are described in Travé et al. (2000).

## 5.2 $\delta^{18}O$ and $\delta^{13}C$ Values of Host Rock and Calcite Veins

The $\delta^{18}O$ values of the host rock (lacustrine limestones and carbonate fraction in the marls) range from -7.1‰ to -4.7‰ PDB, and the $\delta^{13}C$ values vary between -5.7‰ and -3.5‰ PDB (Fig. 5, Table 1), which are consistent with freshwater limestones and meteoric calcite cements (Veizer, 1992).

The oxygen and carbon isotopic composition of the calcite cements filling the diff rent fractures (from –8.6 to -7.7‰ PDB and from -5.3 to -4.1‰ PDB, respectively) plot within a much narrower range of values than the isotopic composition of the host rocks adjacent to the fractures.

The calcite veins filling the upper mineralised backthrust have more negative isotopic values than the values of their adjacent host rock by 1.8 to 2.3‰ for $\delta^{18}O$ values and 0.4 to 0.9 ‰ for $\delta^{13}C$. The calcite veins filling small fractures in the upper mineralised backthrust footwall have $\delta^{18}O$ values between 1.6 and 1.9‰ and $\delta^{13}C$ values 0.4‰ more negative than the values of their adjacent host rock. The calcite veins filling the lower mineralised backthrust have $\delta^{18}O$ values between 2.2 and 2.5‰ more negative and $\delta^{13}C$ values between 0.3 and 0.4 more positive than the values of their adjacent host rock. The calcite veins filling minor faults in the forethrust footwall have $\delta^{18}O$ values between 3.8 and 3.9‰ and $\delta^{13}C$ values 1.1‰ more negative than the values of their adjacent host rock. The calcite veins filling small fractures in the less deformed areas have $\delta^{18}O$ values between 1.3 and 2.0‰ more negative than the values of their adjacent host rock and $\delta^{13}C$ values between 0.4 and 0.5‰ more positive than their adjacent host rock (Fig. 5, Table 1).

The oxygen isotopic compositions of all the calcite veins in the El Guix anticline are consistent with precipitation from a meteoric or an evolved meteoric fluid (Hudson, 1977; Marshall, 1992). The carbon isotopic compositions of the calcite veins with values within the same range of values as the calcite fraction of the host rocks indicate that the carbon for these veins proceeded from homogenising C derived from the host rock.

The values of the calcite cements in microfracture stages 1, 2, and 3 are all within the same range, between -8.6‰ and -7.7‰ PDB for $\delta^{18}O$ and between -5.3‰ to -4.1‰ PDB for $\delta^{13}C$, indicating a common fluid responsible for calcite precipitation during the diff rent stages.

## 5.3 $^{87}Sr/^{86}Sr$ Values of Host Rock and Calcite Veins

The calcite fractions of the host rock have a $^{87}Sr/^{86}Sr$ ratio ranging from 0.70865 to 0.70941 (Fig. 6, Table 1). The calcite veins in the diff rent fractures have a $^{87}Sr/^{86}Sr$ ratio varying from 0.70887 to 0.70911. The halite and gypsum samples from the underlying Cardona Salt Formation have values ranging from 0.70793 to 0.70797, which are slightly higher than the late Eocene-early Oligocene marine signal ranging from 0.7077 to 0.7079 (Hess et al., 1986; Hess et al., 1989; Denison et al., 1993).

Although the host rocks adjacent to the diff rent fractures have a diff rent $^{87}Sr/^{86}Sr$ ratio, the calcite veins in the diverse fractures plot within a narrow range of values, averaging those of the host rocks, as has been already obseved for the stable isotope values. An $^{87}Sr/^{86}Sr$ versus $\delta^{13}C$ plot gives a well defined correlation of the 7 values (r=0.91), with the two extreme values determined by the calcite fraction of the host rocks and the intermediate values defined by the

calcite veins in the fractures. This correlation indicates that the $^{87}Sr/^{86}Sr$ isotopic composition of the calcite veins in the fractures was sourced within the adjacent host rocks. Influences from the underlying Cardona Salt Formation are not reflected by the $^{87}Sr/^{86}Sr$ ratio of the calcite veins in the fractures.

### 5.4 Elemental Geochemistry

The elemental composition of the fluid from which calcite precipitated was determined from the elemental geochemistry of the calcite cements (Travé et al., 2000). The results show that most of the mineralising fluids for the analysed calcite veins have Mg/Ca molar ratios lower than 0.2, which is consistent with a formation water composition. Only three samples from the small fractures in the upper mineralised backthrust footwall have a Mg/Ca molar ratio higher than 0.2, which is consistent with a meteoric water composition. The Sr/Ca molar ratio of the mineralising fluid for calcite veins in the small fractures in the upper mineralised backthrust footwall, in the lower mineralised backthrust, and in the minor faults in the forethrust footwall is higher than 0.007, which is consistent with a formation water composition. The Sr content in the upper mineralised backthrust and in the small fractures in the less deformed areas is always below the detection limit. Most of the mineralising fluids for calcite veins in the upper mineralised backthrust have a Ca/Fe molar ratio higher than 1000, consistent with a meteoric water composition. By contrast, most of the mineralising fluids for calcite veins in the small fractures in the upper mineralised backthrust footwall, in the lower mineralised backthrust, in the minor faults in the forethrust footwall and in the small fractures in the less deformed areas have a Ca/Fe molar ratio lower than 1000, consistent with a formation water composition. Most of the mineralising fluids for calcite veins in all the studied samples have a Mn/Ca molar ratio higher than 0.0002, consistent with a meteoric water composition. The presence of Na is restricted to the upper mineralised backthrust, the small fractures in the upper mineralised backthrust footwall and the lower mineralised backthrust, indicating that only the backthrust array allowed precipitation from a fluid derived from the underlying Cardona Salt Formation.

To sum up, the fluid precipitating the calcite veins in the upper mineralised backthrust was basically consistent with a meteoric origin, whereas the fluid precipitating the calcite veins in the other fractures was basically consistent with a formation water origin. However, the presence of Na in all the fractures of the backthrust array including the upper mineralised backthrust indicates that these fractures also served as a pathway for a fluid which has been in contact with the underlying evaporites.

Diff rences between the three microfracture stages are not evident in the Mg/Ca, Ca/Fe and Mn/Ca molar ratios of the precipitating fluids. However, the presence of Sr and Na only in microfracture stage 2 indicates that during this stage the topographycally-driven fluid flow, arrived deeper, at the underlying Cardona Salt Formation.

The intergranular porosity of the host rock was filled during precipitation of cement in microfracture stage 3.

### 5.5 Fluid Circulation During the Late Development of Continental Fold-and-Thrust System

In the El Guix area, meteoric fluids, with high Fe/Mn and Fe/Mg ratios, without Na and Sr, enriched with $^{13}C$ and with low $^{87}Sr/^{86}Sr$ with respect to their host rock were widely distributed in the structure throughout all its evolution, within a relatively open palaeohydrological system. Evolved meteoric fluids, with lower Fe/Mn and Fe/Mg ratios, with Na and Sr, depleted in $^{13}C$ and with high $^{87}Sr/^{86}Sr$ with respect to their host rock were only present during thrust faults development within a relatively closed palaeohydrological system. The underlying evaporites acted as the lower boundary of the aquifer.

## 6 Discussion and Conclusions

In this section we summarize the existing links between fluid history and tectonic evolution in the South-Pyrenean foreland basin during the Tertiary. Th se relationships show a mutual interaction, also detected in other foreland basins, which are working together during the forwards propagation of tectonic stresses through the sedimentary basin. The understanding of the role of fluids before, during and after thrusting as well as the role of the thrust faults as conduits or seals for fluid migration are key questions to be addressed. Understanding this interaction may help to clarify and better explore the migration of hydrocarbons in fold-and-thrust belts and foreland basins.

#### Timing of Thrusting, Fluid Migration, Thermal History and Relationships With Hydrocarbons

Fluid migration has been detected through the entire Tertiary evolution of the South-Pyrenean thrust front as revealed by the three analysed examples (Atiart-

Arro, L'Escala and El Guix) with diff rent ages of deformation (Table 2).

In Atiart-Arro and El Guix sites, a similar sequence of microstructures, formed during the main compressive event, has been recognised. Microfracture stage 1 is characterised by sediment disaggregation showing that vein formation began in poorly lithifi d sediment. Microfracture stage 2 corresponds to the main episode of shear vein formation indicating a change in the deformation mechanism due to progressive induration of the host sediment. Microfracture stage 3 indicates a decrease of intensity of compressive deformation and could correspond to local extensional rebound in the veins that form tabular bodies more competent than the host-sediment host sediment.

Because veins of diff rent generations in a same outcrop show a similar chronology of microfractures, we conclude that sediment induration was restricted to the vicinity of the vein, probably due to cement precipitation in the vein, and that the sediment away from the veins remained poorly lithifi d during the whole deformation sequence.

In both areas, Atiart-Arro and El Guix, geochemical characteristics of the calcite cements in the three microfracture stages are similar, and the main episode of bulk host-rock cementation by calcite occurred after compressive deformation. This occurred because in this foreland basin the front of deformation advanced within the soft ediment early after its deposition.

Diff rently, in the L'Escala site, the sequence of microfractures coeval with thrusting has not been recognised. In this outcrop, the analysed structures correspond to pre-thrusting fractures, probably developed coevally to the first shortening events characterised by intense spread layer-parallel shortening (Casas et al., 1996; Sans et al., 2003), syn-thrusting fractures, and post-thrusting fractures. As occurred in the other two areas, the main episode of bulk host-rock cementation by calcite occurred after the main compressive deformation, i.e., synchronously to the development of the post-thrust strike-slip faults.

The sequence of calcite veins in the Atiart-Arro fold-and-thrust system developed under submarine thrusting during early-middle Eocene times. The sequence of calcite veins in the L'Escala thrust precipitated during middle-late Eocene times under transitional marine-continental conditions. And finally, the calcite veins filling the fractures at the El Guix anticline precipitated during early Oligocene times under continental conditions (Fig. 10). Th se continental conditions were established in the entire basin at the Priabonian (late Eocene), when the uplift of the western Pyrenees closed up the foreland connection to the Atlantic (e.g., Vergés et al., 1995; Serra-Kiel et al., 2003a, b).

A good correlation for the $^{87}Sr/^{86}Sr$ values of the calcite veins in the Arro fold (Atiart-Arro fold-and-thrust system) with the Eocene marine waters is observed (Fig. 6). However, the samples from L'Escala

**Table 2.** Evolution pattern of the structures, microstructures, fluids, hydrologic regime, and fluid type. The "*" indicate the main thrusting event. The arrows indicate chronology.

| | Evolution pattern | | | | |
|---|---|---|---|---|---|
| | **Structures** | **Fractures** | **Fluids** | **Hydrologic system** | **Fluid type** |
| **Atiart-Arro** | 3 thrusts faults<br>1 footwall syncline | 3 stages of microfractures in syn-thrust shear veins | local and deep derived hot fluids (in the syncline)<br>+<br>larger distance*<br>(in the thrusts) | closed (in the syncline) and more open* (in the thrusts) | Seawater to formation water (in the syncline)<br>and<br>Deep derived + meteoric + local transformations*<br>(in the thrusts) |
| **L'Escala** | pre-thrust diaclases<br><br>3 thrust faults<br><br>post-thrust sinistral faults<br><br>post-thrust NW-SE diaclases | 3 stages of macrofractures (pre, syn and post-thrust) | no fluid recorded<br>⇩<br>larger distance*<br>⇩<br>local<br>⇩<br>larger distance | open*<br>⇩<br>closed<br>⇩<br>open | Meteoric*<br>⇩<br>Evolved meteoric<br>⇩<br>Hot meteoric or deeply derived |
| **El Guix** | forethrusts<br>backthrusts | 3 stages of microfractures in syn-thrust shear veins | local<br>⇩<br>larger distance*<br>⇩<br>local | closed<br>⇩<br>open*<br>⇩<br>closed | Meteoric<br>⇩<br>Evolved meteoric*<br>⇩<br>Meteoric |

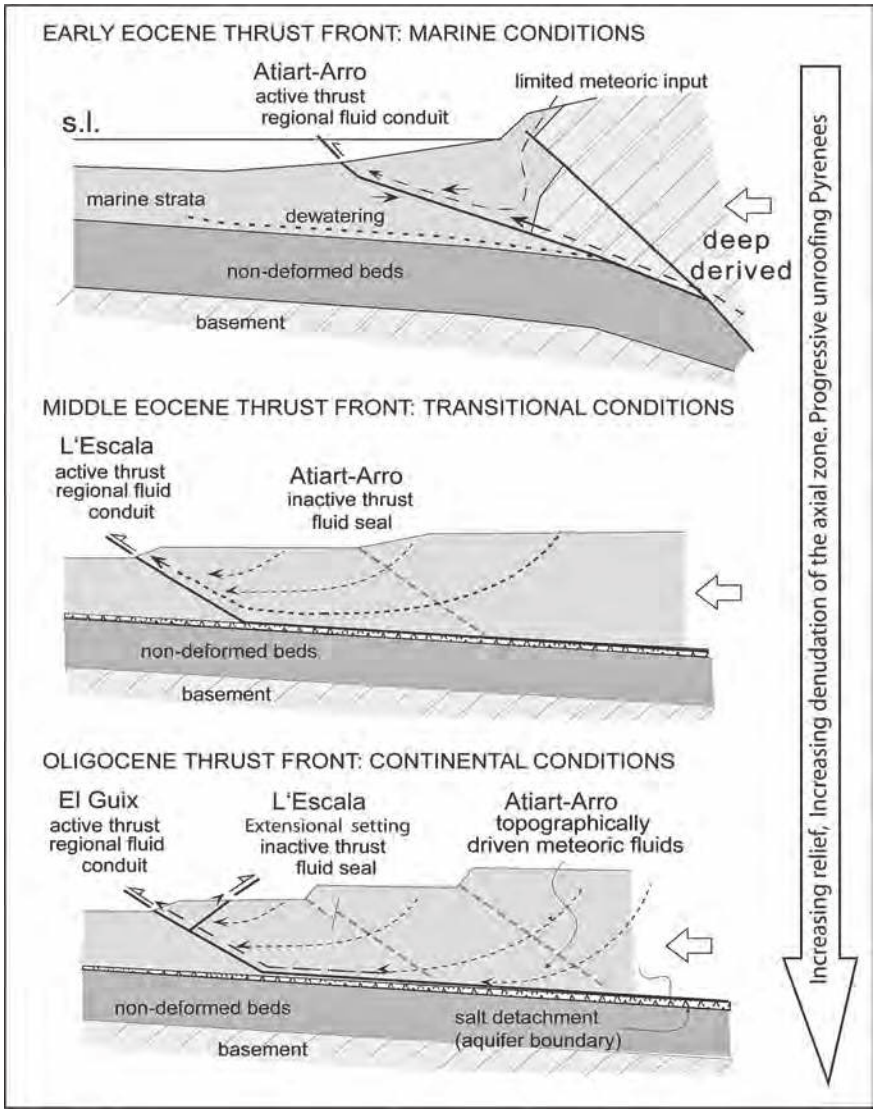


**Fig. 10.** Model of fluid flow pattern during the geodynamic evolution of the Southern Pyrenean fold-and-thrust belt. The different studied areas are drawn in the different sections although they did not develope at the same time or within the same section. They should be regarded as "type" outcrops.

and El Guix show a progressive more radiogenic $^{87}Sr/^{86}Sr$ ratio and more depleted $\delta^{13}C$ values.

The $^{87}Sr/^{86}Sr$ ratios in lake water and in non marine carbonates reflect the ages and Rb/Sr ratios of the rocks exposed to weathering in the drainage basin in which carbonates were deposited (Neat et al., 1979). Thus, these $^{87}Sr/^{86}Sr$ ratios may increase by exposure of crystalline basement rocks to weathering (Brass, 1976), and the stratigraphic variations of the $^{87}Sr/^{86}Sr$ ratios of non marine carbonate rocks can be used to detect changes in the geology or hydrology of the drainage basin (Neat et al., 1979). Similarly, the $^{87}Sr/^{86}Sr$ ratios of calcite cements have been attributed to reflect the isotopic composition of Sr release into the pore fluid by diff rent Rb-bearing rocks and minerals (Stanley & Faure, 1979). On the other hand, the homogeneity of $^{87}Sr/^{86}Sr$ ratios of calcite cements in a lithological unit is a reflection of the rate of flow of formation water through the lithologic unit or aquifer. Relatively rapid water flow tends to make $^{87}Sr/^{86}Sr$ ratios homogeneous, whereas stagnant conditions caused by low permeability or a low hydrostatic gradient permit local variations to develop in the isotopic composition of Sr of calcite cements (Stanley & Faure, 1979).

The progressive increase in the $^{87}Sr/^{86}Sr$ ratio observed in the studied samples (Fig. 6), from the Arro-Atiart thrust system to L'Escala thrust and, finally, to the El Guix anticline, is interpreted to have been produced by a progressive increase of exposure of crystalline basement rocks to weathering and progressive erosion of the Axial Zone of the belt. An increase of the basement clasts, reaching up to about 70% at the top of a middle Eocene succession, has been observed from the lower Lutetian to middle Bartonian succes-

sion of the Ripoll syncline, in the northern part of the eastern Catalan basin (Ramos et al., 2002).

All the host rock samples of the three studied regions show a great overlap of the $\delta^{18}O$ values, around -6.5‰ PDB (from -8.2 to -4.7‰) (Fig. 5). The calcite cements within the fractures in the three studied regions also show a great overlap of the $\delta^{18}O$ values, around -8.5‰ PDB (from -9.6 to -5.9‰). Systematically, the calcite veins of each locality show a shift around -2 ‰ (always lower than -3.9‰) of the $\delta^{18}O$ values with respect to their adjacent host rock. Conversely, the host rock samples of the three studied regions show distinct $\delta^{13}C$ values (from -5.7 to -3.5‰ at El Guix, from -3.3 to -0.7‰ at Atiart-Arro and from -0.8 to 0‰ at L'Escala). The $\delta^{13}C$ values of the calcite cements within the fractures in the three studied regions are all comprised from -5.3 to -0.4‰. In Atiart-Arro and L'Escala regions they show a major overlap of the values, whereas at El Guix the calcite cements show more depleted $\delta^{13}C$ values than in the former areas (Figs. 5 and 6). In all the cases the maximum diff rence between the calcite cement in the fracture and their adjacent host rock is lower than 2.3‰ for $\delta^{13}C$.

In the three studied regions, calcite cement within the host rock precipitated later than in the syn-compressive veins, in a more evolved stage of the deformation history, when the sediment was more indurated. That means that in the earlier stage of deformation the fractures permeability was higher than the host rock permeability even when the porosity within the host rock was still important. In the Atiart-Arro and L'Escala outcrops the $\delta^{18}O$ and $\delta^{13}C$ values of the host rock probably is a mixture of the marine components and the calcite cements precipitated after the main compressive event, with more negative $\delta^{18}O$ values. The lower $\delta^{13}C$ values of the El Guix (both host rocks and calcites cements in veins) could be indicative of the increase of meteoric waters involved in the system, as also deduced from the $^{87}Sr/^{86}Sr$ ratios. This progressive depletion of the $\delta^{13}C$ values of host rock and calcite cements have also been observed in the Atiart-Arro region when comparing the four diff rent outcrops, with possible higher meteoric influences in the structures located closer to the emerged parts of the belt (Travé et al., 1998).

Hot temperature of fluids moving through the fractures during thrusting seems to be coherent with two additional results. In the Atiart-Arro example, microthermometry of fluid inclusions give temperatures between 157ºC and 183ºC (Travé et al., 1998), which are too high for the constrained burial depth between a few hundred of metres and 3 km (Travé et al., 1998). Temperatures between 120ºC and 145ºC have also been reported in calcite veins from the lower Eocene Armancies carbonates (Caja et al., 2006) located in the northern flank of the Ripoll syncline (Fig. 2), which developed coeval to Bellmunt Formation deposition, and which were buried about 3 km (Vergés et al., 1998). So, with a geothermal gradient of 30ºC km-1, that is slightly high for foreland basins, the observed temperatures for the fluids are higher than the ones resulting from only burial depths.

So, we interpret that the thrust-fault zones acted as drains for the fluids derived from both the emerged part of the belt (meteoric fluids) and deeper settings of the thrust systems (footwall dewatering and hot ascending fluids).

This fault control on the fluid system was related to the architecture of the fold-and thrust belt, itself controlled by the organisation of the stratigraphy. Indeed, the main sole thrust of the wedge is located within evaporites (salt or gypsum) horizons, either in the Triassic (Ainsa), the middle Eocene (l'Escala) or the upper Eocene (El Guix), according to the distribution of the various depocentres (Séguret, 1972; Vergés et al.1992). Th se evaporite detachment levels were barriers for deep fluids migrating from the underlying basement, whereas thrusts within the wedge may have drained laterally deep fluids originating from the hinterland thrust basement units forming the Axial Zone. Thus, the hot and high radiogenic fluids that arrived at the thrust front most probably correspond to originally meteoric fluids involved in topographically-driven flow between the Axial Zone relief and the thrust front, and that could interact at depth with the Axial Zone thrust basement before migrating upward through the frontal thrusts.

Other than the thrust fault zones, the only stratigraphic level potentially capable to drain the fluids at a regional scale is the Paleocene to middle Eocene limestone unit below the detritic basin-fill (cf. Fig. 3A for Ainsa, and Fig. 7 for L'Escala and El Guix). Th se limestones are sealed upward by marly or evaporite horizons and may have drained deep fluids toward the foreland, preventing them to go further upward in the tectonic wedge. Nevertheless, in the Ainsa area, these limestones are also present in the Cotiella nappe, where they could drain meteoric fluids toward the frontal thrusts in the detritic basin-fill (Fig. 3A). By contrasts, the detritic units, which constitute the main part of the wedge and its foreland are constituted by lenticular bodies of sandstones and conglomerates embedded within marly units. Th se bodies may have acted as local drains, but could not compete with the thrust faults for long-distance circulation within the wedge.

The close interaction between thrusting and fluids can be used to decipher the timing of fluid migration. As in many fold-and-thrust belts, the thrust system propagates towards the foreland involving younger undeformed strata. We suggest that the thrusts are not only the primary conduits for fluids moving from up-

| | Factors controlling the fluid dynamics | | | |
|---|---|---|---|---|
| | Type of structure | Type of microstructure | Existence of high relief | Type of host rocks |
| Atiart-Arro | *** | *** | * | * |
| L'Escala | *** | - | ** | - |
| El Guix | *** | *** | *** | * |

**Table 3.**
Factors controlling the fluid dynamics in the three studied areas.

lifted internal areas of the belt to buried external regions of the foreland, but also that the fluids also migrate through time along the propagating thrust system, carrying hot fluids from deeper areas of the thrust system.

Diff rent structures, mesostructures and microstructures were embedded by fluids of diff rent origin and composition (i.e., dewatering of connate waters, diff rent degree of interaction with meteoric waters, hot ascending fluids, fluids having interacted with salts, etc.), showing an important coupling of thrust geometry and fluid composition. Specifically, the evolution of the nature of the fluids and of their interactions with the host rocks are consistent with the evolution of the South-Pyrenean thrust front from deep submarine (Atiart-Arro) to mixed shallow marine - continental (L'Escala), and eventually to intra-mountainous continental (El Guix), coevally to the increase of relief forming and Palaeozoic rock exhumation and erosion in the Axial Zone of the belt (Table 3). The type of structure/microstructure and the existence or not of a high relief seems to be the main factors controlling the fluid dynamics (Table 3), whereas the host rock type do not seem to have played a specific role.

Evidences of oil seep or hydrocarbon bearing fluid inclusions have not been observed in the three studied regions, however an interesting point in the Southern Pyrenean belt is in the northern flank of the Ripoll syncline where the lower part of the Armancies Formation is a good hydrocarbon source rock and presents many oil shows along more than 100 km of E-W trending outcrops. A recent study of the calcite cements filling fractures in the Armancies Formation reveals the presence of two main generations of cements (Caja et al., 2006). The first is attributed to the synthrusting event whereas the second, which presents oil inclusions, evidences hydrocarbon migration through the Armancies Formation coeval with this late calcite cement precipitation. The petrological and geochemical characters of this second generation of calcite cements allow us to correlate them to the post-thrusting calcite cements filling the late extensional fracturesat L'Escala, and ascribed to a late shortening or post-shortening event. The Armancies Formation went into the oil window under burial of about 3 km during deposition of Bellmunt redbeds (Vergés et al., 1998), and was subsequently incorporated into the hanging-wall of the Vallfogona thrust during deposition of the upper part of the Bellmunt redbeds. Consequently, oil generation probably spanned a short period of time before significant thrusting took place and oil migration probably occurred soon after its generation and on limited distance, most of the oil shows being located in the same Armancies formation.

The frontal thrusts studied in this paper were connected to basement thrusts in the inner part of the belt. In the central Pyrenees, the major Gavarnie basement thrust deformed and uplifted the inner part of the Cotiella thrust sheet from the middle Eocene. In the Pic de Port Vieux-Plan de Larri area where the Gavarnie thrust places Palaeozoic strata (Silurian to Devonian sediments) above Permo-Triassic redbeds (Fig. 2), an hypersaline Sr-rich brine was pumped by fault activity from the underlying redbeds (Grant et al., 1990; Banks et al., 1991; McCaig et al., 1995). The flow pattern was highly organised and unidirectional, parallel to the limestone mylonites in the thrust zone. Fluid extraction from the footwall was over short (metric) distances, but flow along the mylonite was rapid and at a kilometre-scale, veins also attesting episodic upward escape of fluid from the fault zone into the hangingwall (McCaig et al., 1995). By contrast, no evidences were found for a significant input of either surface or metamorphic fluids during thrusting. Synchronously, in the Pineta thrust complex that aff cted the Upper Cretaceous-Paleocene cover in the hangingwall of the Gavarnie thrust, the fluid flow system was dominated by two fluids, an external fluid resulting from metamorphic devolatilisation reactions in the underlying silicate rocks (Permo-Triassic slates or Hercynian granodiorites), and a descending connate fluid from the overlying carbonates, both transported at least several kilometres (Bradbury & Woodwell, 1987; Rye & Bradbury, 1988).

Th se works and our results thus show that thrust fault zones are likely to focus long distance transport of fluids pumped from the surrounding rocks and displaced from the basement to the foreland basin.

## Acknowledgements

This work was carried out within the framework of DGICYT grant CGL2006-04860. We acknowledge the

contribution of the Grup Consolidat „Geologia Sedimentària“ 2005/SGR00890. We thank J.A. Muñoz for showing us the l'Escala outcrop, the „Serveis cientificotècnics“ of Barcelona University for the facilities in the electron microprobe and stable isotope analyses, the „C.A.I. de Geocronología y Geoquímica Isotópica of the Universidad Complutense de Madrid“ for the $^{87}Sr/^{86}Sr$ analyses. We greatly appreciate the constructive comments of Rudy Swennen and François Roure, which have improved the manuscript.

## References

Allen, P.A., Homewood, P., Williams, G.D. (1986) Foreland Basins: an introduction. In: Allen, P.A., Homewood, P. (eds.) Foreland Basins. Special Publications of the International Association of Sedimentologists 8: 3–12.

Anadón, P., Colombo, F., Esteban, M., Marzo, M., Robles, S., Santanach, P., Solé Sugrañes, L. (1979) Evolución tectonoestratigráfica de los Catalánides. Acta Geol. Hispánica 14: 242–270.

Arenas, C., Pardo, G. (1999) Latest Oligocene-Late Miocene lacustrine systems of the north-central part of the Ebro Basin (Spain): sedimentary facies model and palaeogeographic synthesis. Palaeogeography, Palaeoclimatology, Palaeoecology 151: 127–148.

Banks, D.A., Davies, G.R., Yardley, B.W.D., McCaig, A.M., Grant, N.T. (1991) The chemistry of brines from an Alpine thrust system in the Central Pyrenees: an application of fluid inclusion analysis to the study of fluid behaviour in orogenesis. Geochim. Cosmochim. Acta 55: 1021–1030.

Bartrina, M.T., Cabrera, L., Jurado, M.J., Guimerà, J., Roca, E. (1992) Evolution of the central Catalan margin of the Valencia through (Western Mediterranean). Tectonophysics 203: 219–247.

Beaumont, C., Muñoz, J. A., Hamilton, J., Fullsack, P. (2000) Factors controlling the Alpine evolution of the central Pyrenees inferred from a comparison of observations and geodynamical models. Journal of Geophysical Research 105: 8121–8145.

Bethke, C.M., Marshak, S. (1990) Brine migrations across North America — the plate tectonics of groundwater. Annual Review of Earth and Planetary Sciences 18: 287–315.

Bitzer, K., Travé, A., Carmona, J.M., Calvet, F. (1998) Fluid flow in foreland basins during emplacement of thrust sheets: modelling the south-Pyrenean Ainsa basin. Bull. Soc. Géol. France 5: 627–634.

Bradbury, H.J., Woodwell, G.R. (1987) Ancient fluid flow within foreland terrains. In: Goff, J.C., Williams, B.P.J. (eds.). Fluid flow in sedimentary bsins and aquifers. Geological Society Special Publication 34: 87–102.

Brass, G.W. (1976) The variation of the marine $^{87}Sr/^{86}Sr$ ratio during Phanerozoic time: interpretation using flux model. Geochimica et Cosmochimica Acta 40: 721–730.

Buatier, M., Travé, A., Labaume, P. Potdevin, J.L. (1997) Dickite related to fluid-sediment interaction and deformation in Pyrenean thrust-fault zones. Eur. J. Mineral. 9: 875–888.

Budai, J.M. (1985) Evidence for rapid fluid migration during deformation, Madison Group, Wyoming and Utah Overthrust Belt. In: Longman, M.W., Shanley, K.W., Lindsay, R. F., Eby, D.E. (eds.). Rocky Mountain Carbonate Reservoirs – A Core Workshop. Soc. Econ. Paleont. Miner. Core Workshop, 7: 377–407, Tulsa.

Burke, W.H., Denison, R.E., Hetherington, E.A., Koepink, R.B., Nelson, H.F., Orro, J.B. (1982) Variation of sea-water $^{87}Sr/^{86}Sr$ throughout Phanerozoic time. Geology 10: 516–519.

Burkhard, M., Kerrich, R. 1988. Fluid regimes in the deformation of the Helvetic nappes, Switzerland, as inferred from stable isotope data. Contrib. Miner. Petrol, 99: 416–429.

Caja, M.A., Permanyer, A., Marfil, R., Al-Aasm, I.S., Martín-Crespo, T. (2006) Fluid flow record from fracture-fill calcite in the Eocene limestones from the South-Pyrenean Basin (NE Spain) and its relationship to oil shows. Journal of geochemical exploration 89: 27–32.

Campani M., Jolivet M., Labaume P., Brunel M., Monié P., Arnaud N., 2005. Denudation kinematics of an orogenic prism: integrated thermochronology and tectonic study in the W-Central Pyrenees (France-Spain). Joint Earth Science Meeting « Thrust Belts and Foreland Basins », Société Géologique de France – Sociedad Geologica de Espana, 14–16 décembre 2005, Rueil-Malmaison.

Calvet, F., Travé, A., Roca, E., Soler, A., Labaume, P. (1996) Fracturación y migración de fluidos durante la evolución tectónica neógena en el Sector Central de las Cadenas Costero Catalanas. Geogaceta 20: 1715–1718.

Casas, J. M., Durney, D., Ferret, J., Muñoz, J. A. (1996) Determinación de la deformación finita en la vertiente sur del Pirineo oriental a lo largo de la transversal del río Ter. Geogaceta 20: 803–805.

Cerling, T.E. (1984) The stable isotopic composition of modern soil carbonate and its relationship to climate. Earth planet. Sci. Lett. 71: 229–240.

Cerling, T.E., Quade, J., Wang, Y. Bowman, J.R. (1989) Carbon isotopes in soils and palaeosols as ecology and palaeoecology indicators. Nature 341: 138–139.

Choukroune, P., and ECORS team (1989) The ECORS Pyrenean deep seismic profile reflection data and the overall structure of an orogenic belt. Tectonics 8: 23–39.

Claypool, G.E., Holser, W.T., Kaplan, I.R., Sakai, H., Zak, I. (1980) The age curves of sulfur and oxygen isotopes in marine sulfate and their mutual interpretation. Chem. Geol. 28: 199–260.

Coney, P. J., Muñoz, J. A., McClay, K. R., Evenchick, C. A. (1996) Syntectonic burial and post-tectonic exhumation of the southern Pyrenees foreland fold-thrust belt. Journal Geological Society, London 153: 9–16.

Cosgrove, J. W. (1993) The interplay between fluids, folds and thrusts during deformation of a sedimentary succession. Journal of Structural Geology 15: 491–500.

Denison, R.E., Koepnick, R.B., Fletcher, A., Dahl, D.A., Baker, M.C. (1993) Re-evaluation of early Oligocene, Eocene, and Paleocene seawater strontium isotope ratios using outcrop samples from the U.S. Gulf Coast. Paleoceanography 8: 101–126.

DePaolo, D. J., Ingram, B.L. (1985) High-resolution stratigraphy with strontium isotopes. Science 227: 938–941.

Dietrich, D., McKenzie, J.A., Song, H. (1983) Origin of Calcite in syntectonic veins as determined from carbon-isotope ratios. Geology 11: 547–551.

Ferket H., Swennen R., Ortuño-Arzate S., Cacas M.C., Roure F., 2004. Hydrofracturing in the Laramide foreland fold-and-thrust belt of Eastern mexico. In Swennen R., Roure F., Granath J., eds., Deformation, fluid flow and reservoir appraisal in foreland fold-and-thrust belts, AAPG Hedberg Series, Memoir, 1, 133–156.

Fitzgerald, P. G., Muñoz, J. A., Coney, P. J., Baldwin, S. L. (1999) Asymmetric exhumation across the Pyrenean orogen: implications for the tectonic evolution of a collisional orogen: Earth And Planetary Science Letters 173: 157–170.

García-Castellanos, D., Vergés, J., Gaspar-Escribano, J., Cloetingh, S. (2003) Interplay between tectonics, climate, and fluvial transport during the Cenozoic evolution of the Ebro Basin (NE Iberia): Journal of Geophysical Research 108: B7, 2347, doi: 10.1029/2002JB002073.

Garven, G. (1985) The role of regional fluid flow in the genesis of the Pine Point deposit, Western Canada sedimentary basin. Economic Geology 80: 307–324.

Garven, G. (1989) A hydrogeologic model for the formation of the giant oil sands deposits of the Western Canada Sedimentary Basin. Ameriacan Journal of Science 289: 105–166.

Garven, G. (1995) Continental scale groundwater flow and geologic processes. Annual Review of Earth and Planetary Sciences 23: 89–117.

Ge, S., Garven, G. (1992) Hydromechanical modeling of tectonically driven groundwater flow with application to the Arkoma foreland basin. J. Geophys. Res. 97, B6: 9119–9144.

Ge, S., Garven, G. (1994) A theoretical model for thrust-induced deep groundwater expulsion with application to the Canadian Rocky Mountains. J. Geophys. Res. 99, B7: 13851–13868.

Grant, N.T., Banks, D.A., McCaig, A.M., Yardley, B.W.D. (1990) Chemistry, source, and behavior of fluids involved in Alpine thrusting of the Central Pyrenees. J. Geophys. Res. 95: 9123–9131.

Hess, J., Stott, L.D., Bender, M.L., Kennett, J.P., Schilling, J.-G. (1989). The Oligocene marine microfossil record: age assessments using strontium isotopes. Paleoceanography 4: 655–679.

Hess, J.; Bender, M.L.; Schilling, J.G. (1986) Evolution of the ratio of strontium-87 to strontium-86 in seawater from Cretaceous to present. Science 231: 979–984.

Hubbert, M. K., Rubey, W. W. (1959) Role of fluid pressure in the mechanics of overthrust faulting. Geological Society of America Bulletin 70: 115–205.

Hudson, J.D. (1977) Stable isotopes and limestone lithification. J. Geol. Soc. London 133: 637–660.

Hudson, J. D., Anderson, T. F. (1989) Ocean temperatures and isotopic compositions through time. Transactions of the Royal Society of Edinburgh 80: 183–192.

Juez-Larré, J., Andriessen, P.A.M. (2006) Tectonothermal evolution of the northeastern margin of Iberian since the breakup of Pangea to present, revealed by low-temperature fission-track and (U-Th)/He thermochronology. A case history of the Catalan Coastal Ranges. Earth and Planetary Science Letters 243: 159–180.

Katz, A., Sass, E., Starinsky, A., Holland, H.D. (1972) Strontium behaviour in the aragonite–calcite transformation: an experimental study at 40–98°C. Geochim. Cosmochim. Acta 36: 481–496.

Koepnick, R.B.; Denison, R.E.; Burke, W.H.; Hetherington, E. A.; Nelson, H.F.; Otto, J.B.; Waite, L.E. (1985) Construction of the seawater $^{87}Sr/^{86}Sr$ curve for the Cenozoic and Cretaceous: Supporting data. Chem. Geol., Isot. Geosci. Sect., 58: 55–81.

Kyser, T.K., Kerrich, R. (1990) Geometry of fluids in tectonically active crustal regions. In: Nesbitt, B.E (ed.). Short Course on Fluids in Tectonically Active Regimes of the Continental Crust. Mineralogical Association of Canada, 18: 133–230, Vancouver.

Longstaffe, F.J. (1993) Meteoric water and sandstone diagenesis in the Western Canada Sedimentary Basin. In: Horbury, A.D., Robinson, A.G. (eds.). Diagenesis and basin development. American Association of Petroleum Geologists. Studies in Geology, 36: 49–68.

Machel, H.G., Cavell, P.A. (1999) Low-flux, tectonically-induced squeegee fluid flow ("hot flash") into the Rocky Mountain Foreland Basin. Bulletin of Canadian Petroleum Geology 47: 510–533.

Marquer, D., Burkhard, M. (1992) Fluid circulation, progressive deformation and mass-transfer processes in the upper crust: the example of basement-cover relationships in the External Crystalline Massifs, Switzerland. Journal of Structural Geology 14: 1047–1057.

Marshall, J. D. (1992) Climatic and oceanographic isotopic signals from the carbonate rock record and their preservation. Geological Magazine 129: 143–160.

Martínez-Peña, B., Casas Sainz, A. M. (2003) Cretaceous-Tertiary tectonic inversion of the Cotiella Basin (southern Pyrenees, Spain): International Journal of Earth Sciences (Geol Rundsch), 92: 99–113.

McCaig, A.M., Wayne, J.M., Marshall, J.D., Banks, D., Henderson, I. (1995) Isotopic and fluid inclusion studies of fluid movement along the Gavarnie thrust, Central Pyrenees: reaction fronts in carbonate mylonites. Am. J. Sci. 295: 309–343.

Mead, G.A., Hodell, D.A. (1995) Controls on the $^{87}Sr/^{86}Sr$ composition of seawater from the middle Eocene to Oligocene: Hole 689B, Maud Rise, Antarctica. Paleoceanography 10: 327–346.

Meigs, A. J., Vergés, J. Burbank, D. W. (1996) Ten-million-year history of a thrust sheet: Geological Society of America Bulletin 108: 1608–1625.

Muchez, P., Slobodnik, M., Viaene, W. A., Keppens, E. (1995) Geochemical constraints on the origin and migration of palaeofluids at the northern margin of the Variscan foreland, soutern Belgium. Sedimentary Geology 96: 191–200.

Muñoz, J. A. (1992) Evolution of a continental collision belt: ECORS-Pyrenees crustal balanced section, in McClay, K. R. (ed.) Thrust Tectonics: London, Chapman & Hall, p. 235–246.

Muñoz, J. A., Martínez, A., Vergés, J. (1986) Thrust sequence in the Spanish eastern Pyrenees. Journal of Structural Geology 8: 399–405.

Mutti, E., Séguret, M. and Sgavetti, M. (1988) Sedimentation and deformation in the Tertiary sequences of the southern Pyrenees: AAPG Mediterranean Basins Conference, p. 169.

Neat, P. L., Faure, G., Pegram, W.J. (1979) The isotopic composition of strontium in non-marine carbonate rocks : The Flagstaff ormation of Utah. Sedimentology 26: 271–282.

Oliver, J. (1986) Fluids expelled tectonically from orogenic belts: their role in hydrocarbon migration and other geologic phenomena. Geology 14: 99–102.

Palmer, M.R.; Elderfield, H. (1985) Sr isotope composition of sea water over the past 75 Myr. Nature, 314: 526–528.

Puigdefàbregas, C., Muñoz, J. A. Marzo, M. (1986) Thrust belt development in the Eastern Pyrenees and related depositional sequences in the southern foreland basin, in Allen, P. A. Homewood, P. (eds.), Foreland basins, Special Public. of the International Association of Sedimentologists 8: 229–246.

Puigdefàbregas, C., Muñoz, J. A., Vergés, J. (1992) Thrusting and Foreland Basin Evolution in the Southern Pyrenees, in

McClay, K. R. (ed.), Thrust Tectonics, Chapman & Hall, p. 247–254.

Qing, H., Mountjoy, E.(1992) Large-scale fluid flow in the Middle Devonian Presqu'ile barrier, Western Canada Sedimentary Basin. Geology 20: 903–906.

Ramos, E., Busquets, P., Vergés, J. (2002) Interplay between longitudinal fluvial and transverse alluvial fan systems and growing thrusts in a piggyback basin (SE Pyrenees). In Marzo, M., Muñoz, J. A., Vergés, J. (eds.) Sedimentary Geology on Growth Strata, Sedimentary Geology 146: 105–131.

Roure, F., Choukroune, P., Berastegui, X., Muñoz, J. A., Villien, A. M., Thereon, P., Bareyt, M., Séguret, M., Cámara, P., Déramond, J. (1989) ECORS deep seismic data and balanced cross sections: Geometric constraints on the evolution of the Pyrenees: Tectonics 8: 41–50.

Roure, F., Carnevali, J.O., Gou, Y. and Subieta, T. (1994) Geometry and Kinematics of the North Monagas thrust Belt (Venezuela). Marine and Petroleum Geology 11: 347–362.

Roure, F., Swennen, R., Schneider, F., Faure, J.L., Ferket, H., Guilhaumou, N., Osadetz, K., Robion, P., Vandeginste, V. (2005) Incidence and importance of tectonics and natural fluid migration on reservoir evolution in foreland fold-and-thrust belts. Oil & Gas Science and Technology – Rev. IFP 60: 67–106.

Rye, D.M., Bradbury, H.J. (1988) Fluid flow in the crust: an example from a Pyrenean thrust ramp. American Journal of Science 288: 197–235.

Sans, M., Vergés, J. (1995) Fold development related to contractional salt tectonics: southeastern Pyrenean thrust front, Spain, in Jackson, M. P. A. Roberts, D. G. Snelson, S. (eds.), AAPG Memoir 65 on Salt Tectonics: a global perspective, Chapter 18: 369–378.

Sans, M., Vergés, J., Gomis, E., Parés, J.M., Schiatarella, M., Travé, A., Calvet, F., Santanach, P., Doulcet, A. (2003) Layer parallel shortenning in salt-detached folds: constraint on cross-section restoration. Tectonophysics 372: 85–104.

Séguret, M. (1972) Etude tectonique des nappes et séries décollées de la partie centrale du versant sud des Pyrénées, Série géologie structurale, n°2, Montpellier, Publications de l' Université des Sciences et Techniques du Languedoc (Ustela).

Serra-Kiel, J., Travé, A., Mató, E., Saula, E., Ferràndez, C., Busquets, P., Tosquella, J., Vergés, J. (2003a) Marine and transitional Middle/Upper Eocene Units of the Southeastern Pyrenean Foreland Basin (NE Spain). Geologica Acta 1: 177–200.

Serra-Kiel, J., Mató, E., Saula, E., Travé, A., Ferràndez, C., Àlvarez-Pérez, G., Busquets, P., Samsó, J.M., Tosquella, J., Frnaquès, J., Romero, J., Barnolas, A. (2003b) An inventory of the Marine and Transitional Middle/Upper Eocene Deposits of the Southeastern Pyrenean Foreland Basin (NE Spain). Geologica Acta 1: 201–232.

Shackleton, N. J., Kennett, J. P. (1975) Paleo-temperature history of the Cenozoic and the initiation of Antarctic glaciation: oxygen and carbon isotope analyses in DSDP Sites 277, 279 and 281. Initial Reports of the Deep Sea Drilling Project, 29: 743–755.

Sinclair, H.D., Gibson, M., Naylor, M., Morris, R.G. (2005) Asymetric growth of the Pyrenees revealed through measurement and modelling of orogenic fluxes. American Journal of Science 305: 369–406.

Stanley, K.O., Faure, G. (1979) Isotopic composition and source of strontium in sandstone cements: The High Sequence of Wyoming and Nebraska. J. Sed. Petr. 49: 45–54.

Travé, A., Labaume, P., Calvet, F., Soler, A. (1997) Sediment dewatering and pore fluid migration along thrust faults in a foreland basin inferred from isotopic and elemental geochemical analyses (Eocene south-Pyrenees, Spain). Tectonophysics 282: 375–398.

Travé, A., Labaume, P., Calvet, F., Soler, A., Tritlla, J., Buatier, M., Potdevin, J.L., Séguret, M., Raynaud, S., Briqueu, L. (1998) Fluid migration during Eocene thrust emplacement in the south Pyrenean foreland basin (Spain): an integrated structural, mineralogical and geochemical approach. In: Mascle, A., Puigdefàbregas, C., Luterbacher, H.P., Fernàndez, M. (eds.), Cenozoic Foreland Basins of Western Europe. Geol. Soc. London, Spec. Publ. 134: 163–188.

Travé, A., Calvet, F., Sans, M., Vergés, J., Thirlwall, M. (2000) Fluid history related to the Alpine compression at the margin of the south-Pyrenean Foreland basin: the El Guix anticline. Tectonophysics 321: 73–102.

Veizer, J. (1992) Depositional and diagenetic history of limestones: stable and radiogenic isotopes. In: Clauer, N., Chaudhuri, S. (eds.), Isotopic Signatures and Sedimentary Records. Lecture Notes in Earth Sciences 43: 13–48. Springer, Berlin.

Veizer, J., Hoefs, J. (1976) The nature of $O^{18}/O^{16}$ and $C^{13}/C^{12}$ secular trends in sedimentary carbonate rocks. Geochimica et Cosmochimica Acta 40: 1387–1395.

Vergés, J., Muñoz, J.A., Martinez, A. (1992) South Pyrenean fold-and-thrust belt : Role of foreland evaporitic levels in thrust geometry, in McClay, K.R. (ed.), Thrust Tectonics, London, Chapman et al., p. 255–264.

Vergés, J., Millán, H., Roca, E., Muñoz, J. A., Marzo, M., Cirés, J., den Bezemer, T., Zoetemeijer, R., Cloetingh, S. (1995) Eastern Pyrenees and related foreland basins: Pre-, syn- and post-collisional crustal-scale cross-sections. In Cloetingh, S., Durand, B., Puigdefàbregas, C. (eds.) Marine and Petroleum Geology 12: 903–916.

Vergés, J., Burbank, D. W. (1996) Eocene-Oligocene Thrusting and Basin Configuration in the Eastern and Central Pyrenees (Spain), in Friend, P. F. Dabrio, C. J. (eds.), Tertiary Basins of Spain. The Stratigraphic Record of Crustal Kinematics, Cambridge University Press. World and Regional Geology 6: 120–133.

Vergés, J., Marzo, M., Santaeulària, T., Serra-Kiel, J., Burbank, D. W., Muñoz, J. A., Giménez-Montsant, J. (1998) Quantified vertical motions and tectonic evolution of the SE Pyrenean foreland basin., In Mascle, A., Puigdefàbregas, C., Luterbacher, H. P., Fernàndez, M. (eds.), Cenozoic Foreland Basins of Western Europe, London, Geological Society Special Publications 134: 107–134.

Vergés, J., Fernàndez, M. Martínez, A. (2002) The Pyrenean orogen: pre-, syn-, and post-collisional evolution, in Rosenbaum, J. G. Lister, G. S. (eds.), Reconstruction of the evolution of the Alpine-Himalayan Orogen, Journal of Virtual Explorer 8: 55–84.

Yeh, H.W., Savin, S.M. (1977) Mechanisms of burial metamorphism of argillaceous sediments: 3. O-isotope evidence. Geological Society of America Bulletin 88: 1321–1330.